
Entanglement Entropy, the Multi-scale Entanglement Renormalisation Ansatz and Lifshitz Field Theories

Institute for Theoretical Physics
Utrecht University

Author: Kevin Kavanagh
Supervisor: Prof. Dr. Stefan Vandoren

15 December 2017



Universiteit Utrecht

Abstract

In this thesis we will summarise recent developments in tensor network methods and extend results for entanglement entropy using cMERA in Lifshitz field theories. After a brief recounting of the important aspects of entanglement entropy we will present a description of pertinent tensor networks. This will include both matrix product states (MPS) and the multi-scale entanglement renormalisation ansatz (MERA). We will recount previous area law results for the entanglement entropy in these ansätze. Following this we will continue to discuss MERA and in particular its continuous realisation (cMERA). Finally we apply this cMERA framework to free field theories and extend known results to the case of field theories with anisotropic scaling, that is, Lifshitz field theories. In particular we find a new result for the entanglement entropy of fermionic theories with anisotropic scaling.

Acknowledgements

While this thesis has been written by one person, it would never have been made without the support of many more. Firstly, I would like to thank my supervisor Stefan for his assistance and guidance on this journey without which I may have been lost at times. This thesis not only marks the end of a Master but also the end of my time in Utrecht. I thank all of those who have made this city a home during my time here, in particular Efi, Pieter and Damjan. For making the study and research far easier I thank my colleagues and friends: Adriana, António, Emma, Domingo to mention but a few.

Lastly, most importantly, I thank my family. Without your support and unending encouragement over these last years and, indeed, far before I would never have been able to make it to this point.

Contents

1	Introduction	2
2	Entanglement Entropy	4
2.1	Entanglement in Quantum Mechanics	4
2.2	Entanglement Entropy	5
2.3	Area Laws	7
3	Tensor Networks	8
3.1	Diagrams and Notation	8
3.2	Matrix Product States	10
3.2.1	EE Bound for MPS	13
3.2.2	Examples of MPS states	14
3.3	Tree Renormalisation	15
3.4	MERA	18
3.4.1	MERA Examples	22
3.4.2	Properties of the MERA	22
3.4.3	EE Bound for MERA	24
4	AdS/MERA	27
4.1	cMERA	31
4.1.1	Scalar Field Theory	33
4.1.2	An Emergent Metric	36
5	cMERA and Lifshitz Theories	38
5.1	Lifshitz Scaling	38
5.2	Scalar Field	38
5.3	Dirac Field	46
5.4	Lifshitz Dirac I	49
5.5	Lifshitz Dirac II	50
6	Conclusion	53
A	Quantum Information	54
A.1	Qubits	54
A.2	Quantum Gates	54
A.3	Quantum Circuits	55
A.4	States and Representations	56
B	Bibliography	58

Chapter 1

Introduction

Almost since the inception of quantum mechanics, the notion of entanglement in quantum systems has been a source of interest. Initially there was some scepticism as evidenced by Einstein-Podolsky-Rosen's paradoxical thought experiment [1] which cast doubt on quantum mechanics as a true description of reality. However almost 30 years later Bell famously put forward a rebuttal [2] which would eventually allow entanglement to be verified as a physical fact many years later. Since these beginnings the study of entanglement and its measure, entanglement entropy, has simply grown and grown. One area of interest is the study of entanglement entropy in many-body quantum mechanical systems. However, the study of many-body physics is often hindered by the intractability of the associated calculations owing to the fact that one will often be faced with an exponential scaling of variables with system size. A way to overcome this problem is to make approximations. Often this comes in the guise of mean-field theory or similar methods, however, in this thesis we examine tensor network methods. In simple terms tensor networks are representations of many body states. The methods which use these networks are several variational ansätze from which one can determine the ground state of a system and properties thereof. The variational parameters are the tensors themselves which comprise the network.

In recent years a wealth of material has been produced on the topic of tensor networks. This can be attributed to the wide range of applications that physicists from disparate areas have found and developed. It can be said that in 1992 White [3, 4] initiated this field with a numerical method known by DMRG (Density Matrix Renormalization Group). Although some numerical methods will be mentioned in this thesis the focus will be on analytic results arising from these developments.

Since 1992 a wide variety of tensor networks (TN) have been developed for various different contexts. The DMRG method may be seen diagrammatically via matrix product states (MPS) and their manipulations. This class of TN is particularly suited to 1-dimensional quantum spin systems. For large spin chains direct diagonalization methods for numerical calculations quickly become intractable. DMRG allows for these calculations to become tractable by using the framework of matrix product states to make enormous savings on memory and computation time by reducing the number of relevant degrees of freedom in the problem.

Moreover, these MPS were generalized to higher dimensions. Projected Entangled Pair States or PEPS are a class of 2D tensor networks which are essentially a 2 dimensional analogue of matrix product states. [5] Although many of the higher dimensional tensor networks do not share the numerical benefits of their lower dimensional counterparts they are of theoretical interest.

For this thesis our primary focus is another class of tensor networks which have properties that make them of special interest to the study of entanglement entropy for low dimensional systems. These so called MERA networks are $(d + 1)$ -dimensional networks which are used to

describe states on a d -dimensional lattice. The numerical benefits of these networks are found in $d = 1, 2$ but higher dimensional MERA networks are also of interest. Our focus in this thesis will be the theoretical implications of this Multi-scale Entanglement Renormalisation Ansatz. It has been proposed that the network may be viewed as a discretisation of space-time. [6]

There are a number of properties which make the MERA network of particular interest to us. Firstly, as a tensor network we should be able to extract numerical results which were not so readily available or possible by previous methods. Moreover, the ansatz is suitable for the study of scale invariant theories, that is, many body quantum systems at critical points. Using a slightly modified version of the network the MERA is also a quantum circuit which unitarily evolves an IR state to a UV state. Then, taking a broader view of the ansatz, the network describes a renormalization group flow from a ultraviolet state/theory to an infrared state/theory. Then two aspects which we will examine in this thesis are more recent developments. It has been conjectured that the MERA network yields a discrete form of Anti-de Sitter space-time. [6] We will present this conjecture and a related proposal in which a continuous MERA framework which may be used to study emergent space-time from quantum field theories [7, 8],

Later we will extend this cMERA proposal to Lifshitz field theories, often referred to as theories with anisotropic scaling. That is, field theories in which the scaling of time and space dimensions are not equal. In effect the modification we will see is that usual spatial derivative term we find in the free field theories will be replaced by a higher derivative term. The number of derivatives will be denoted by ν which is referred to as the dynamical critical exponent. The reason we explore this avenue of research is to probe theories with long-range entanglement and to determine properties of non-relativistic theories at quantum critical points. How a higher derivative corresponds to longer range entanglement can be seen by examining the theory on a lattice [9]. Moreover, by exploring this area we hope to find general results for various values of the dynamical critical exponent such that one can say something meaningful about the nature of entanglement for Lifshitz field theories. In recent years Lifshitz-type theories have become of increased interest in the areas of gravitation [10, 11], condensed matter theory [12] and fluid dynamics [13, 14].

The structure of the thesis is then as follows, in Chapter 2 we will give a brief introduction to entanglement entropy. We will for the most part only introduce the key concepts that are of use in the subsequent discussions. Following this, in Chapter 3, we will introduce the necessary tools to understand tensor networks with an introduction to matrix product states, real space renormalisation and finally a brief treatment of MERA. In Chapter 4, the proposal which links entanglement renormalisation (MERA) and holography (AdS/CFT) will be introduced. This proposal in itself is an exciting prospect as we see a connection between a real space renormalisation technique originally intended for use in the field of condensed matter becoming linked to the AdS/CFT correspondence in part due to the Ryu-Takayanagi proposal [15, 16]. We will in fact see a manifestation of the RT proposal in the scaling of entanglement entropy of MERA in Chapter 3. In the final Chapter (5), we will reproduce and expand upon recent work in the area of continuous MERA and Lifshitz scaling, yielding results for general dynamical exponent in free field theories.

Chapter 2

Entanglement Entropy

In this thesis the key quantity around which discussion will be focused is the entanglement entropy of a quantum mechanical system. Entanglement itself is one of the basic phenomena of quantum mechanics and the entanglement entropy is a measure of this phenomenon. We will introduce the concept in this chapter in a relatively formal way but the ideas will be crucial throughout the later chapters and will reappear throughout the discussions of tensor networks.

In the context of tensor networks there are several useful resources from Quantum Information Theory [17, 18], which give a more complete picture than will be presented here.

2.1 Entanglement in Quantum Mechanics

The phenomenon of entanglement is seen in the difference between the state spaces of classical and quantum mechanical systems. If we have a system which comprises of multiple subsystems one expects classically that the entire system will be describable by a direct sum of the individual subspaces. In the mathematical description of a quantum mechanical system this is equivalent to the state space or Hilbert space of the system being factorisable as a tensor product of the individual Hilbert spaces. So if we have two subsystems A and A^c , namely a subsystem A and its complement, then the full space can be expressed as $\mathcal{H} = \mathcal{H}_A \otimes \mathcal{H}_{A^c}$. Or in terms of the states:

$$|\Psi\rangle = |\psi\rangle \otimes |\phi\rangle, \quad (2.1)$$

where $|\psi\rangle \in \mathcal{H}_A$ and $|\phi\rangle \in \mathcal{H}_{A^c}$. This would correspond to subsystem A being in state $|\psi\rangle$ and subsystem A^c being in state $|\phi\rangle$. However in quantum mechanics this is not always true as the tensor product space is comprised of all linear combinations of product states so if we have a set of bases $\{|\psi_a\rangle\}$, $\{|\phi_b\rangle\}$ then a generic state will be expressed as:

$$|\Psi\rangle = \sum_{a,b} M_{ab} |\psi_a\rangle \otimes |\phi_b\rangle \in \mathcal{H}, \quad (2.2)$$

but it may arise that no states $|\psi\rangle$, $|\phi\rangle$ exist such that:

$$\sum_{a,b} M_{ab} |\psi_a\rangle \otimes |\phi_b\rangle = |\psi\rangle \otimes |\phi\rangle. \quad (2.3)$$

In other words the state of the system is not in a product state but rather it is an entangled state. A simple example of such a state is given by one of the Bell state describing a state of two qubits¹:

$$|\beta_{00}\rangle = \frac{1}{\sqrt{2}}(|00\rangle + |11\rangle). \quad (2.4)$$

¹If one is unfamiliar with the notation or nomenclature of quantum information used here, further explanation is given in the appendix.

This particular state is not factorisable as the tensor product of two single qubit states. Hence we say that it is entangled.

More concretely entanglement is the name given to a purely quantum mechanical correlation between systems. Say in spontaneous pair production from the vacuum of spin- $\frac{1}{2}$ particles. By spin conservation both are created with opposite spin. Then if one of the particles is observed say as a spin up particle then the other particle is known to be in a spin down configuration. As such there is a correlation between the particles even if they are separated in space. In a sense it seems that the measurement of one particle affects the subsequent measurement outcome of the other particle. This action at a distance concept was viewed with some scepticism initially [1]. However through the work of Bell [2] entanglement has subsequently been verified experimentally allowing for acceptance of this phenomenon as a fundamental aspect of quantum mechanics.

Since these beginnings the study of entanglement has become an enormous topic of interest in physics. Particularly in the fields of condensed matter and quantum information theory. However these are not the only fields where it appears, it is also of interest in the areas of black hole physics, and holography which this thesis will touch upon.

2.2 Entanglement Entropy

Given that entanglement appears in such a wide range of research it becomes essential to have a quantitative measure for the amount of entanglement in a system or more accurately between two subsystems. The relevant measure is the *entanglement entropy*.

Before defining the entanglement entropy we should remind ourselves of the relevant object used to define the entropy, namely the (reduced) density matrix of a (sub-)system. The density matrix is a necessary tool when there is some uncertainty about a given state. We say that the state is thereby in a mixed state, or an ensemble of pure states. This can be due to the system in question being in thermal equilibrium or indeed if we have a system comprised of several entangled subsystems, in which case the subsystems must be treated as being in mixed states regardless of the state of the larger system.

In mathematical terms for a pure state vector $|\psi\rangle$ the density matrix is defined as the linear operator:

$$\rho = |\psi\rangle\langle\psi|. \quad (2.5)$$

Using this definition quantum mechanics may be reformulated in terms of density operators rather than states such that the Schrödinger equation becomes the von Neumann equation:

$$i\hbar\frac{\partial\rho}{\partial t} = [H, \rho]. \quad (2.6)$$

For a mixed state the density matrix is defined as a linear combination of pure state density matrices in a similar sense to taking linear combinations of pure states to express a multiple qubit state for example. So the density matrix is then:

$$\rho = \sum_k p_k |\psi_k\rangle\langle\psi_k|. \quad (2.7)$$

The coefficients p_k are classical probabilities of the system being in some k -th state. A state is said to be pure if $\rho^2 = \rho$.

The reason for using density matrices in the study of entanglement entropy is precisely due to the presence of entanglement since it leaves a gap in the knowledge of a subsystem. For example if one has an entangled system but has only experimental access to a subsystem then

the information of the subsystem is incomplete due to the state space of the whole system being non-factorisable.

Now to set up the definition of the entanglement entropy consider the system previously described. We have a full system described by the density matrix ρ , but we are interested in a subsystem A described by ρ_A . As before we can say that the whole system is $\mathcal{H}_A \otimes \mathcal{H}_{A^c}$ where A^c is the complement of A as before. For example this could be a wire or spin chain of N sites split in the middle with A being one half and A^c being the remainder but the discussion holds in generality. Then the density matrix of A is defined by ρ where all the degrees of freedom in A^c are traced out. This is expressed as:

$$\rho_A = \text{Tr}_{A^c}(\rho). \quad (2.8)$$

In other words we sum over the degrees of freedom which we know nothing about, leaving us with only the information that can be known of the subsystem A . Even if ρ is a pure state ρ_A can be mixed, this defines entanglement. If it is the case that there is no entanglement between A and A^c then ρ factorises completely as $\rho_A \otimes \rho_{A^c}$ similar to when we looked at state vectors.

To quantify the entanglement we define the entanglement entropy. This is known as the von Neumann entropy which is the quantum mechanical version of classical Shannon entropy. It is defined as:

$$\begin{aligned} \mathcal{S}(\rho) &= -\text{Tr}(\rho \log \rho), \\ &= -\sum_{k=1}^N p_k \log(p_k), \end{aligned} \quad (2.9)$$

where p_k are the eigenvalues of ρ and ρ is a matrix of dimension $N \times N$. A pure state corresponds to a density matrix with eigenvalue equal to 1 and hence has zero entanglement entropy. A maximally mixed state corresponds to a density matrix with all eigenvalues equal to $1/N$ and hence $\mathcal{S}(\rho) = \log N$.

A couple of useful relations are worth mentioning at this point as we will make use of them in later discussions. The first is subadditivity of entanglement entropy. Given a system with full density matrix ρ split into a subsystem and its complement as previously described the entropies of the subsystems sum to be greater or equal to the entropy of the total system. That is:

$$\mathcal{S}(\rho) \leq \mathcal{S}(\rho_A) + \mathcal{S}(\rho_{A^c}). \quad (2.10)$$

A way to understand this is if we consider the measure of entropy as a measure of our lack of knowledge of a system then naturally one expects the whole system to contain more information than the individual subsystems when examined separately.

Another relation of note is the Araki-Lieb inequality [19], which is in effect the full triangle inequality:

$$|\mathcal{S}(\rho_A) - \mathcal{S}(\rho_B)| \leq \mathcal{S}(\rho) \leq \mathcal{S}(\rho_A) + \mathcal{S}(\rho_{A^c}), \quad (2.11)$$

where A and B are different choices for splitting the system and A^c is again the complement of A . One should note that the choice of subsystem is important as different subsystems will not necessarily have the same entanglement with the remainder of the system for some given ρ . Indeed they may be entirely different. The key point is that the entanglement is not an inherent feature of a state but is dependent on the way in which we examine the parts of the state.

2.3 Area Laws

If one takes a generic quantum mechanical state, the entanglement entropy of that state will be proportional to the volume of the subsystem/subinterval one examines. This agrees with our classical notion of entropy, the entropy of a system is proportional to the number of degrees of freedom and hence the volume of the system at hand.

However, not all states share this property. An important class of states are those whose entanglement entropy follows an area law. Essentially one finds that the entropy is proportional to the boundary of the subsystem at hand. This phenomenon appears in lattice systems and in continuous systems [20]. Indeed for MERA networks this aspect is characteristic of the tensor network ansatz.

Suppose we have a d -dimensional quantum system. Then if we examine the entanglement entropy of a region A of side length l , whether a hypercubic region of a lattice or a space-time, if the system obeys an area law then we expect the entropy to behave as:

$$\mathcal{S}(\rho_A) \propto l^{d-1}. \quad (2.12)$$

So in effect the entropy is proportional to the boundary of the region in question as opposed to the total number of degrees of freedom in the system. For a random quantum state in general the entropy may scale with the volume of the region, meaning that as for classical entropy the entanglement entropy will scale as an extensive quantity.

It has been found that the ground states of local, gapped Hamiltonians in many cases obey this area law [21]. General criteria for when a state will or will not obey an area law is not currently known but various examples have been shown. Regardless, local interactions are evidently an important ingredient. As we will see this aspect will be a natural part of the tensor networks which we will examine.

As we will see in later discussions an important exception to the area law are 1-dimensional systems at critical points. In this scenario it has been found that a logarithmic correction to the areal law manifests itself. If we naively consider (2.12) one may expect that the system will exhibit:

$$\mathcal{S}(\rho_A) \propto l^{1-1} = \text{constant}. \quad (2.13)$$

However, in actual fact what is found for 1-dimensional critical systems is the following²

$$\mathcal{S}(\rho_A) \propto \log(l). \quad (2.14)$$

In more generality the logarithmic violation is:

$$\mathcal{S}(\rho_A) \sim \mathcal{O}(l^{d-1}) \log(l). \quad (2.15)$$

More specific examples such as for a conformal field theories will be presented at a later point where we will see that MPS and MERA states at critical points exhibit area laws.

²Often in this case we will still refer to the 1-dimensional log law as the area law.

Chapter 3

Tensor Networks

In this chapter we will introduce tensor network states with explanation of the notation and diagrammatic representation of these states. Our main focus will be on a simple type of tensor network namely a Matrix Product State (MPS), followed by tree tensor networks (TTN) and later the Multiscale Entanglement Renormalisation Ansatz (MERA) which will be more important to this thesis and will be given an expanded treatment in later chapters.

The field of tensor networks can be said to have been initiated by the work of White [3] where the Density Matrix Renormalisation Group (DMRG) method was first proposed. Since then however the field has expanded greatly [4] with a huge number of more recent developments. Moreover, many different kinds of tensor networks have been proposed for use in different situations [5, 6, 20, 22–35]. Initially these works were motivated by the difficulty in simulating many-body quantum systems. The issue being that with a large number of constituent particles the number of degrees of freedom in a system usually scales exponentially and as a result the computational time and processing power required renders the problems intractable. However, with tensor network states it is possible to reduce the number of necessary variables greatly allowing for meaningful and accurate results to be found by reasonable means.

3.1 Diagrams and Notation

Before describing individual tensor networks it is first useful to understand the notation and nomenclature used. The diagrammatic forms of tensor networks are represented using the graphical tensor notation of Penrose, an excellent description of which is found in the book *Road to Reality* [36], further discussion in various areas can be found elsewhere [37].

Usually when we wish to express physics mathematically we make use of some compact, abstract notation. For example, rather than representing a velocity by a direction and speed we use the language of vector calculus. When we study manifolds in general relativity we use compact index notation so that rather than manipulating large matrices we can write down tensors such as:

$$g_{\mu\nu}, \mathcal{R}_{\sigma\gamma\alpha\beta}, \Gamma_{\alpha\beta}^{\mu}. \quad (3.1)$$

However, at some point even this notation becomes cumbersome. Instead we can represent tensors by a graphical notation in which different tensors maybe denoted by different geometric shapes and indices may be represented by lines (or legs) emanating from these shapes so that the tensorial structure remains evident but the cumbersome notation is removed.

We continue with some simple examples. The metric tensor for example is usually written as $g_{\mu\nu}$ in most situations. Moreover if we contract two metric tensors we know the result is a delta function:

$$g^{ab} g_{bc} = \delta_c^a, \quad (3.2)$$

where the Einstein summation convention is used to contract over the repeated indices thus simplifying the more complete expression:

$$\sum_{b=0}^d g^{ab} g_{bc} = \delta_c^a, \tag{3.3}$$

if we have $(d + 1)$ -dimensions. Using Penrose's graphical tensor notation however this becomes the simply a vertical line as shown below:

$$g^{ab} = \cap, \quad g_{ab} = \cup, \quad \delta_b^a = |, \\ g^{ab} g_{bc} = \cup \cap = | = \delta_c^a.$$

While this may not yet seem worthwhile the real benefit is seen from more complicated products of tensors with several repeated indices. For example, say we have a rank $(1,1)$ tensor which we wish to contract with a vector. Usually we may write this as, say, $\Gamma_\beta^\alpha v_\alpha$. The graphical version of this is shown below.

$$\Gamma_\beta^\alpha v_\alpha = \begin{array}{c} \beta \\ | \\ \boxed{\Gamma} \\ | \\ \alpha \\ \circledast v \end{array}. \tag{3.4}$$

If we like we can dream up more complicated products and find their graphical representation quite readily and vice-versa. Take for instance:

$$\Delta^{\alpha\beta\gamma\rho} \Psi_{\alpha\beta} \Sigma_{\gamma}^{cd} \Pi_{ab}^e \Omega_{d\rho}. \tag{3.5}$$

This is already quite a nasty expression with only five tensors. If we have 10 or 20 tensors it will become unwieldy to manage the indices as we will see shortly for MPS or MERA. So instead this expression can be drawn as shown in the next figure. After contracting the repeated indices we can see immediately from the figure that in the end we have a rank $(2,0)$ tensor without need for examining all of the indices to verify which are summed or not summed.

$$\begin{array}{c} \boxed{\Delta} \\ | \quad | \\ \boxed{\Psi} \quad \triangle{\Sigma} \\ | \quad | \quad | \\ \triangle{\Pi} \quad \circledast{\Omega} \\ | \quad | \end{array} = \Phi^{ce}. \tag{3.6}$$

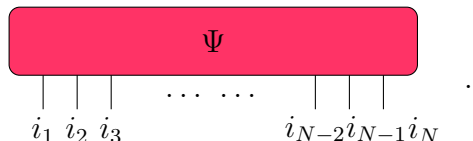
We will leave the discussion here and begin to apply this graphical notation to quantum mechanical systems in order to build up tensor networks.

3.2 Matrix Product States

The key notion in constructing tensor networks comes from the usual representation of a quantum state. For example, suppose we want to determine some properties of an N -site spin chain. If we are only concerned for the moment with the spin then we can write the state as:

$$|\Psi\rangle = \sum_{i_1 \dots i_N} \psi^{i_1 \dots i_N} |i_1 \dots i_N\rangle, \quad (3.7)$$

where the summation variables run over all the possible spin states. In diagrammatic notation the tensor in question is given as:



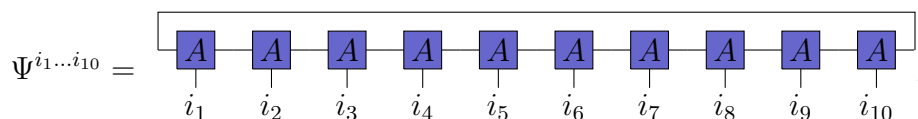
$$\Psi \quad (3.8)$$

Even if there are only 2 spin states, up/down, then the number of variables in the object $\psi^{i_1 \dots i_N}$ is 2^N . So for even quite small systems, say a 1-d wire with $N = 50$, we can have 10^{15} variables to worry about. Quickly then numerical work becomes intractable. The way around this is to find a better representation of the state in question, specifically one in which it is possible to systematically make an approximation to the state in question.

Since the state space of a quantum mechanical system will be a vector space we will view the elements of the vector space and the linear operators which act on them as tensors of various rank. So, for example, vectors (or *kets*) are rank-(1,0) tensors and dual vectors (or *bras*) are rank-(0,1) tensors. Then if indeed we have an N -site state then we can view it as a rank-($N,0$) tensor. The network aspect of the tensor network state comes from our choice or ansatz of the tensor in question. As you can see in the previous section, a tensor of particular rank may have any number of digrammatic representations since there may be several tensors within the network or graph which are contracted. Since this is the case ansatz solutions are proposed.

The first of these is the Matrix Product State. It is applied to 1 dimensional systems. If the system in question has N -sites then the MPS for the state will be comprised of N tensors of rank 3¹.

Take then the state above, described in the usual quantum mechanical notation. What we would like to do is to decompose the $\psi^{i_1 \dots i_N}$ is 2^N tensor into a network of N simpler objects. In graphical form we can see the N leg ψ tensor in the figure. Below we see the MPS representation of $|\Psi\rangle$ for the case of $N = 10$ with periodic boundary conditions.



$$\Psi^{i_1 \dots i_{10}} = \quad (3.9)$$

Notice that in the same way that the ψ tensor has N free legs so too does the MPS state, where each free leg corresponds to a state vector index for the relevant lattice site. In all detail, the mathematical expression for this MPS is:

$$|\Psi\rangle = \sum_{\alpha_1 \dots \alpha_N=1}^{\chi} \sum_{i_1 \dots i_N=1}^d A_{\alpha_2}^{i_1 \alpha_1} A_{\alpha_3}^{i_2 \alpha_2} \dots A_{\alpha_N}^{i_{N-1} \alpha_{N-1}} A_{\alpha_1}^{i_N \alpha_N} |i_1 i_2 \dots i_N\rangle, \quad (3.10)$$

usually the summation will be left implicit.

¹For periodic boundary conditions, the boundary tensors will be of rank 2, with the rest of rank 3.

Ignoring the free indices the remaining indices are contracted in the same way as a matrix product, hence the name. These contracted indices are known as *bonds* in tensor network literature. While the physical indices, i_k , run over the number of on site degrees of freedom, the bond indices, α_k , do not. Instead they run from 1 up to what is called the *bond dimension*. If we may take the bond dimension, χ , as large as necessary then this ansatz is in fact a representation for 1 dimensional systems [30, 38]. This however has a similar problem to the usual representation since for an arbitrary state the bond dimension will scale exponentially in the number of sites. It's also worth noting that the MPS representation is not a unique representation, there may be several MPS for a single state.

So at the moment it seems that we haven't gained anything however there is a class of states for which the bond dimension can be "small"². One way of understanding what this bond dimension can be is to consider how to obtain the MPS representation directly from a given $\psi^{i_1 \dots i_N}$. A procedure may be performed on an $(N, 0)$ rank tensor whereby a Schmidt decomposition is performed on the tensor N times, leaving one with an MPS.

The procedure begins by performing a singular value decomposition between the first index of the large tensor and the remaining $N - 1$ indices. This process is iterated until we are left with N matrices. The matrices which we obtain by this method will be of dimension $\chi \times \chi$ and will be unitary.

As an example suppose we would like to split an N -site system into two pieces. So the full Hilbert space, \mathcal{H} , of the system is split into two subspaces, $\mathcal{H}_A \otimes \mathcal{H}_B$. The dimension of these subspaces is then d^m and d^{N-m} respectively where d is the physical dimension, e.g. number of spin states per site. If we propose that the Hilbert spaces have orthonormal bases $|i\rangle, |j\rangle$ respectively then a state of the system may be expressed as:

$$|\Psi\rangle = \sum_{i,j} \Psi^{ij} |i\rangle |j\rangle. \quad (3.11)$$

The singular value decomposition of the matrix Ψ is given by:

$$\Psi = U s V^\dagger, \quad (3.12)$$

where U and V are unitary matrices of dimensions $m \times m$ and $(N-m) \times (N-m)$ respectively. The matrix s then is a diagonal matrix of dimension $m \times (N-m)$. All the entries of s are non-negative real numbers, where $s_{11} \geq s_{22} \geq \dots \geq s_{mm}$. They are known as the singular values of Ψ . Replacing Ψ in the original expression we have:

$$|\Psi\rangle = \sum_{i,j} \sum_k U_{ik} s_{kk} V_{kj}^* |i\rangle |j\rangle = \sum_k s_{kk} |a_k\rangle |b_k\rangle, \quad (3.13)$$

where $|a_k\rangle$ and $|b_k\rangle$ are the transformed bases according to:

$$|a_k\rangle = \sum_i^m U_{ik} |i\rangle; |b_k\rangle = \sum_j^{N-m} V_{kj}^* |j\rangle. \quad (3.14)$$

The second form in the transformed bases is what is known as the Schmidt decomposition. Pictorially, we can see the procedure below for the case of $N = 4$. One should understand here which legs correspond to which indices. The i index corresponds to the left most leg in the diagram. The j index corresponds to the remaining 3 legs which in the procedure are grouped together as one index j running over all the values of i_2, i_3, i_4 . The k index corresponds to the

²The meaning of small here is not precise, it effectively means that the bond dimension won't scale exponentially in number of sites or will be a constant.

bond between U , s and V^\dagger .

$$\Psi \rightarrow U \text{---} s \text{---} V^\dagger. \quad (3.15)$$

A way of understanding this is to consider the Schmidt decomposition as a superposition of many states in which each term is comprised of a product of a basis state of A and a basis state of B weighted by a value s_{kk} . At this point the benefit of an MPS can be demonstrated. From the distribution of the values of s_{kk} we can have some clue to the entanglement between the two systems as before. Suppose that there is one singular value $s_{11} = 1$, evidently this will correspond to a product state $|a_1\rangle |b_1\rangle$. On the other hand if all the singular values are equal, $s_{kk} = 1/\sqrt{m}$, $\forall k$, then we have a maximally mixed state, an equal superposition of all basis states. It is known that the distribution of these singular values decays exponentially for a certain value of k much less than m . In fact for large matrices many of the singular values will in fact be zero, particularly for the types of states which are of interest to us. Then we may make an approximation at this point, by discarding the small or zero valued singular values we can still retain much of the information about the state with a large reduction in the number of variables.

$$|\Psi\rangle \rightarrow |\tilde{\Psi}\rangle = \sum_{k=1}^{\chi \ll m} s_{kk} |a_k\rangle |b_k\rangle. \quad (3.16)$$

In the case of MPS the number of values which are kept is the bond dimension. So in fact the number of variables is reduced from d^N to $\text{poly}(\chi, N)$. So it becomes a much more efficient representation. This decomposition is a central component of the DMRG method. Aside from assisting in numerical methods another way of viewing this reduction in number of variables is by considering the Hilbert space for a generic state. If the bond dimension is left unrestricted then it will scale exponentially with the number of lattice sites and will in fact be equal to the dimension of the full Hilbert space. This situation is sensible since an unrestricted bond dimension allows the MPS to be a faithful representation of the original state so in fact the full Hilbert space should remain [38]. In essence what is happening when the bond dimension is restricted is that we are restricting ourselves to a subspace of the Hilbert space which contains the states that are of interest to us, namely ground states of local gapped Hamiltonians. In comparison to the full Hilbert space of such a Hamiltonian, the subspace containing these states will in fact be small requiring a bond dimension which is not exponential in N but rather may be constant. The appropriate value then of the bond dimension will depend on the states which we aim to represent and the accuracy required to faithfully represent them. By construction an MPS state supports local correlations, that is correlations which decay exponentially, and lead to saturated entropy bounds at large scales. This is due to the nature of the MPS being comprised of nearest neighbour interactions, which can be seen from the structure of the network, since each tensor is linked only to its nearest neighbours.

A note should be made at this point, from the figure and previous discussion it may seem that we have implied that all the matrices which make up an MPS are the same. However, in generality an MPS may be made up of N distinct matrices. Although, in many of the discussions that follow we will focus on states which have translation invariance or are at critical points. In those cases the matrices are restricted to being identical [38].

Another point of interest is that this prescription of splitting a tensor with multiple indices into several tensors each located at an individual site can be applied not only to states but also to operators. Operators may be represented as matrix product operators. This is another key

ingredient in the DMRG method. In that context a local Hamiltonian may be decomposed as a sum of nearest neighbour terms. The interaction then on the state is equivalent to a contraction of the MPS with the MPO. For further discussion on this point see [38].

Using the MPS representation we can readily demonstrate the area law violation of entanglement entropy for matrix product states mentioned in the previous chapter.

3.2.1 EE Bound for MPS

If we have a 1D system of size N described by an MPS, such that $A[k]^i \in M_{\chi \times \chi}$, and take section of size $L < N$, then the entropy of this smaller block has $2 \log_2(\chi)$ as an upper-bound independent of the size L .

$$\begin{aligned} \forall |\psi_{mps}\rangle : A[k]^i \in M_{\chi \times \chi} \forall k, \text{ if } \rho_L = Tr_{s \notin L} |\psi_{mps}\rangle \langle \psi_{mps}|, \\ \implies S(\rho_L) \leq 2 \log_2(\chi) \forall L. \end{aligned}$$

Proof

In general we express an MPS as follows:

$$|\psi\rangle = \sum_{\alpha_1, \dots, \alpha_N=1}^{\chi} \sum_{i_1, \dots, i_N=1}^d A[1]_{\alpha_1}^{i_1} A[2]_{\alpha_1 \alpha_2}^{i_2} \dots A[N-1]_{\alpha_{N-2} \alpha_{N-1}}^{i_{N-1}} A[N]_{\alpha_{N-1}}^{i_N} |i_1 \dots i_N\rangle.$$

Now we split the state into three pieces, a region of length L and the remainder of the system on either side of this region. Define the sections as below:

$$\begin{aligned} |\psi_l\rangle_{\alpha_m} &= \sum_{\alpha_1, \dots, \alpha_{m-1}=1}^{\chi} \sum_{i_1, \dots, i_m=1}^d A[1]_{\alpha_1}^{i_1} A[2]_{\alpha_1 \alpha_2}^{i_2} \dots A[m]_{\alpha_{m-1} \alpha_m}^{i_m} |i_1 \dots i_m\rangle, \\ |\psi_L\rangle_{\alpha_m \alpha_{m+L}} &= \sum_{\alpha_{m+1}, \dots, \alpha_{m+L-1}=1}^{\chi} \sum_{i_{m+1}, \dots, i_{m+L}=1}^d A[m+1]_{\alpha_m \alpha_{m+1}}^{i_{m+1}} \dots A[m+L]_{\alpha_{m+L-1} \alpha_{m+L}}^{i_{m+L}} |i_{m+1} \dots i_{m+L}\rangle, \\ |\psi_r\rangle_{\alpha_{m+L}} &= \sum_{\alpha_{m+L+1}, \dots, \alpha_N=1}^{\chi} \sum_{i_{m+L+1}, \dots, i_N=1}^d A[m+L+1]_{\alpha_{m+L} \alpha_{m+L+1}}^{i_{m+L+1}} \dots A[N]_{\alpha_{N-1}}^{i_N} |i_{m+L+1} \dots i_N\rangle. \end{aligned}$$

Now we may view the state $|\psi\rangle$ as follows:

$$|\psi\rangle = \sum_{\alpha_m, \alpha_{m+L}=1}^{\chi} |\psi_l\rangle_{\alpha_m} |\psi_L\rangle_{\alpha_m \alpha_{m+L}} |\psi_r\rangle_{\alpha_{m+L}}.$$

At this point one would like to find the reduced density matrix of this state ρ_L which will be more easily obtainable using the form above. By definition:

$$\begin{aligned} \rho_L &= Tr_{s \notin L} (|\psi\rangle \langle \psi|), \\ &= \sum_{\substack{\alpha_m, \alpha_{m+L} \\ \alpha'_m, \alpha'_{m+L} \\ \alpha''_m, \alpha''_{m+L}}} \left\langle \psi_{\alpha''_{m+L}}^r \left| \left\langle \psi_{\alpha''_m}^l \left| \psi_{\alpha_m}^l \right\rangle \left| \psi_{\alpha_m \alpha_{m+L}}^L \right\rangle \left| \psi_{\alpha_{m+L}}^r \right\rangle \left\langle \psi_{\alpha'_m \alpha'_{m+L}}^r \left| \left\langle \psi_{\alpha'_m}^L \left| \psi_{\alpha'_m \alpha'_{m+L}}^L \right\rangle \left| \psi_{\alpha'_m}^l \left| \psi_{\alpha'_m}^l \right\rangle \left| \psi_{\alpha'_{m+L}}^r \right\rangle \right. \right. \right. \end{aligned}$$

$$\begin{aligned}
&= \sum_{\substack{\alpha_m, \alpha_{m+L} \\ \alpha'_m, \alpha'_{m+L} \\ \alpha''_m, \alpha''_{m+L}}} \left\langle \psi_{\alpha''_{m+L}}^r \left| \delta_{\alpha''_m \alpha_m} \left| \psi_{\alpha_m \alpha_{m+L}}^L \right\rangle \left| \psi_{\alpha_{m+L}}^r \right\rangle \left\langle \psi_{\alpha'_{m+L}}^r \left| \left\langle \psi_{\alpha'_m \alpha'_{m+L}}^L \left| \delta_{\alpha'_m \alpha'_m} \left| \psi_{\alpha''_{m+L}}^r \right\rangle \right. \right. \right. \right. \\
&= \sum_{\substack{\alpha_m \\ \alpha_{m+L}}} \left| \psi_{\alpha_m \alpha_{m+L}}^L \right\rangle \left\langle \psi_{\alpha_m \alpha_{m+L}}^L \right|.
\end{aligned}$$

From this expected result the argument follows from the definition of the von Neumann entropy. For some density matrix σ we have that $S = \text{Tr}(-\sigma \log_2(\sigma))$.

Naturally then σ will have a set of eigenvalues $\{\lambda_1 \dots \lambda_R\}$ where $R = \text{rank}(\sigma)$. Therefore, $S(\sigma) = -\sum_{k=1}^R \lambda_k \log(\lambda_k)$. The maximum value of this entropy will come from the maximally mixed state which we know to have all eigenvalues equal, $\lambda_k = \frac{1}{R} \forall k$, hence

$$S^{\text{max}}(\sigma) = -\sum_{k=1}^R \frac{1}{R} \log_2\left(\frac{1}{R}\right) = \log_2(R).$$

Then finally for our ρ_L we have that: $\text{rank}(\rho_L) = \chi^2$, where χ is the bond dimension. Thus we obtain the bound:

$$S(\rho_L) \leq 2 \log_2(\chi).$$

Some discussion of this result is of use. Notice that in addition to the expected logarithmic term there is a factor of 2 multiplying the log. From the usual description of an area law one expects to find $|\partial A|$ multiplying the logarithm, where $|\partial A|$ is the size of the boundary of the region in question. From examination of the MPS we can reconcile both of these results. As the MPS is 1-dimensional so the boundary of a region of the MPS must then be of 0-dimension or a constant. By examining the diagram one can see that this corresponds to the number of bonds at the boundary of the region which is in fact 2. If one wishes to isolate a subset of MPS tensors from the remaining network, two bonds would have to be severed.

3.2.2 Examples of MPS states

At this point it is useful to see benefits of the matrix product state representation by way of some simple concrete examples of states that one may know already.

GHZ State

The Greenberger-Horne-Zeilinger (GHZ) state in bra-ket notation is defined as:

$$|GHZ\rangle \equiv \frac{1}{\sqrt{2}} (|000\rangle + |111\rangle), \quad (3.17)$$

on 3 sites and likewise on N sites:

$$|GHZ\rangle \equiv \frac{1}{\sqrt{2}} (|00\dots 0\rangle + |11\dots 1\rangle). \quad (3.18)$$

Rather than having a tensor $\Psi^{i_1 i_2 \dots i_N}$ which contains 2^N variables most of which are zero we can represent this state exactly by constructing an MPS with $\chi = 2$. The matrices which achieve this are:

$$A_0 = \begin{pmatrix} 1 & 0 \\ 0 & 0 \end{pmatrix}, \quad A_1 = \begin{pmatrix} 0 & 0 \\ 0 & 1 \end{pmatrix}, \quad (3.19)$$

where we are using (3.10) to represent the state with the above matrices.

W State

Another state which is of interest for the study of entanglement is the W state defined on N sites as:

$$|W\rangle \equiv |0\dots 001\rangle + |0\dots 010\rangle + |0\dots 100\rangle + \dots |10\dots 00\rangle, \quad (3.20)$$

$$= \sum_{j=1}^N |000\dots 01_j 0\dots 0\rangle. \quad (3.21)$$

This can also be exactly represented by an MPS with $\chi = 2$ defined by the matrices:

$$A_0 = \begin{pmatrix} 1 & 0 \\ 0 & 1 \end{pmatrix}, \quad A_1 = \begin{pmatrix} 0 & 1 \\ 0 & 0 \end{pmatrix}. \quad (3.22)$$

3.3 Tree Renormalisation

So far we have focused on a 1-dimensional tensor network for a 1-dimensional system, the MPS, where each lattice site corresponds to a single tensor. This idea has been generalised also to 2-dimensions via projected entangled pair states [5]. Now, while matrix product states have many benefits as representations of quantum states we can construct tensor networks with more complicated structures which have richer structure. In the same manner that MPS are the tensor network structure for DMRG we can suppose other types of network structures which by construction allow for numerical renormalisation directly.

The usual first example of such a tensor network is known as a tree tensor network or TTN. In much of the literature this is also known as real-space renormalisation or simply coarse-graining. The essential idea is that the tensor network itself performs a coarse graining procedure to the lattice of the quantum system. Then rather than a single tensor per site, many tensors appear at different length scales. The key resources for understanding this section comes from Vidal's original papers introducing real-space renormalisation and MERA by this method [33, 35, 39]. The presentation of TTN follows these references closely.

Real space renormalisation methods truncate the local Hilbert space of a block of sites to reduce the number of effective degrees of freedom. Essentially the initial lattice is group into contiguous blocks of sites which are mapped to an effective lattice containing fewer sites and hence fewer degrees of freedom. We may then consider such a lattice in D spatial dimensions. This may be a lattice of spin- $\frac{1}{2}$ fermions or whatsoever. If the original lattice is denoted by \mathcal{L} then we may express the Hilbert space of this lattice as the following tensor product of finite vector spaces:

$$\mathbb{V}_{\mathcal{L}} \equiv \bigotimes_{s \in \mathcal{L}} \mathbb{V}_s, \quad (3.23)$$

where s are the sites on the lattice, \mathbb{V}_s are the state spaces per site. A block of sites, $\mathcal{B} \subset \mathcal{L}$, within the lattice may be defined in a similar manner as:

$$\mathbb{V}_{\mathcal{B}} \equiv \bigotimes_{s \in \mathcal{B}} \mathbb{V}_s. \quad (3.24)$$

The new effective lattice, \mathcal{L}' , is obtained by mapping these coarse graining these blocks to new sites, $s' \in \mathcal{L}'$. Specifically,

$$\mathbb{V}_{\mathcal{L}'} \equiv \bigotimes_{s' \in \mathcal{L}'} \mathbb{V}'_{s'}, \quad (3.25)$$

where the effective state spaces, $\mathbb{V}'_{s'}$, are subspaces of the block subspaces, $\mathbb{V}'_{s'} \subseteq \mathbb{V}_{\mathcal{B}}$. This subspace is characterised by the mapping of an isometric tensor w ,

$$w : \mathbb{V}'_{s'} \mapsto \mathbb{V}_{\mathcal{B}}, \quad w^\dagger w = \mathbb{I}. \quad (3.26)$$

Then the choice of w is determined by *White's Rule*, which in effect is a choice of w such that the projector defined previously corresponds to the whole support of ρ :

$$P = ww^\dagger = \sum_{\alpha=1}^{\chi} |\Psi_\alpha\rangle \langle\Psi_\alpha|. \quad (3.34)$$

In particular this means that $W^\dagger |\Psi_{GS}\rangle = |\Psi'_{GS}\rangle$ and $WW^\dagger |\Psi_{GS}\rangle = |\Psi_{GS}\rangle$. So in fact by a quick inspection we see that:

$$\begin{aligned} \langle\Psi_{GS}| o_1 o_2 \dots o_k |\Psi_{GS}\rangle &= \langle\Psi_{GS}| W^\dagger W o_1 o_2 \dots o_k W W^\dagger |\Psi_{GS}\rangle \\ &= (\langle\Psi_{GS}| W^\dagger) W o_1 o_2 \dots o_k W (W^\dagger |\Psi_{GS}\rangle) = \langle\Psi'_{GS}| o'_1 o'_2 \dots o'_k |\Psi'_{GS}\rangle. \end{aligned}$$

Then from this we can see that this entire process may be iterated many times, so that we may have a series of increasingly coarse grained lattices in precisely the same manner as shown in the figure of the TTN. At each successive layer we produce a smaller lattice which retains the properties of the ground state. So if we denote the step or layer of coarse graining by τ then we can say as above that:

$$\langle o_1^{(\tau+1)} o_2^{(\tau+1)} \dots o_k^{(\tau+1)} \rangle_{\Psi_{GS}^{(\tau+1)}} = \langle o_1^{(\tau)} o_2^{(\tau)} \dots o_k^{(\tau)} \rangle_{\Psi_{GS}^{(\tau)}}. \quad (3.35)$$

A reasonable question to ask at this point is: how well does the TTN scheme remove short range degrees of freedom? If it is the case that they are not removed effectively then over successive iterations of the TTN they may build up rendering the numerical benefits of the procedure void. As a check we investigate the entanglement of the ground state. Suppose that we have a reduced density matrix for a block of sites on the lattice. Then the rank of this matrix, χ , will depend on the amount of entanglement between the block of sites and the rest of the lattice. Taking the Schmidt decomposition of the ground state we have:

$$|\Psi_{GS}\rangle = \sum_{\alpha=1}^{\chi} \sqrt{\lambda_\alpha} |\Psi_\alpha\rangle \otimes |\Phi_\alpha\rangle, \quad (3.36)$$

where $\{|\Phi_\alpha\rangle\}$ are an orthonormal set of states for the remainder of the lattice. Evidently then if $\chi = 1$ we have a product state and hence no entanglement between the block and the remaining lattice. Evidently for any $\chi > 1$ we have entanglement between the block and the remaining lattice. Moreover the size of χ will directly correspond to the amount of entanglement determined from the von Neumann entropy:

$$\mathcal{S}(\rho) = - \sum_{\alpha=1}^{\chi} p_\alpha \log(p_\alpha). \quad (3.37)$$

The entropy is as usual maximized for a maximally mixed state where $p_\alpha = 1/\chi$, which corresponds to $\mathcal{S}(\rho) = \log(\chi)$. As a result, we always have that $\chi \geq \exp(\mathcal{S})$. For simplicity we take $\chi \approx \exp(\mathcal{S})$ for the remaining discussion. Typically, in 1-dimension, for a block of sites of size l the entanglement entropy increases with l until l is of the same order as the typical correlation length of the system, ξ . At this point it saturates to some bound \mathcal{S}_{max} unless the system is at a quantum critical point, in which case the entropy exhibits a logarithmic divergence.

$$\mathcal{S}(l) \leq \mathcal{S}_{max}, \quad \text{1D non-critical} \quad (3.38)$$

$$\mathcal{S}(l) \approx \frac{c}{3} \log(l), \quad \text{1D critical} \quad (3.39)$$

c in this context is the central charge of the conformal field theory which describes the system at the critical point. More generally in D dimensions we usually find a boundary law as mentioned

previously, $\mathcal{S}(l) \approx \alpha l^{D-1}$ ³. The area law can tell us something of the scaling of χ . We wish to find an expression for the effective dimension $\chi^{(\tau)}$ at a given layer. Noting that a single site on an effective lattice under this TTN scheme supports 3^τ sites on the underlying lattice or $3^{D\tau}$ sites in D dimensions then combining the above bounds with the relation between the entropy and χ we find:

$$\chi^{(\tau)} \leq \chi_{max} \approx e^{\mathcal{S}_{max}}, \quad \text{1D non-critical} \quad (3.40)$$

$$\chi^{(\tau)} \approx l^{c/6} \approx e^\tau, \quad \text{1D critical} \quad (3.41)$$

$$\chi^{(\tau)} \approx e^{\alpha l} \approx e^{e^{\sqrt{\tau}}}. \quad \text{2D} \quad (3.42)$$

Then we can see that evidently a TTN doesn't not remove short range degrees of freedom effectively. In fact there is a build up of these degrees of freedom over the successive iterations of the coarse graining procedure. In effect what is happening here is that starting from a state with only short range entanglement rather than removing some of the associated degrees of freedom they are in fact building up. More precisely the entanglement between sites is treated differently depending on where the sites are located in a block. If the short range degrees of freedom are entangled across the boundary between two blocks then they are not removed and as a result hinder attempts to produce an renormalisation group flow from the original Hamiltonian to the renormalised Hamiltonian. So for instance, two Hamiltonians which differ only in short range details but which describe the same phase of a system will keep these distinguishing features under renormalisation resulting in two different fixed points of the RG flow for the same phase. In some cases in 1-dimension TTN are certainly still of interest but given this RG issue we present another tensor network which will possess the benefits of the previously discussed networks and resolve this issue: the multiscale entanglement renormalisation ansatz (MERA).

3.4 MERA

Similarly to a tree tensor network the multiscale entanglement renormalisation ansatz tensor network also incorporates a coarse graining or real space renormalisation scheme. However, in addition to the isometries that we have already seen an additional type of tensor is built into the structure of the network. In the literature these tensors are referred to as disentanglers. These rank(2,2) tensors, unitary operators, are located at the boundary of the blocks on the lattice, denoted by u . The purpose of these disentangling operators is to rearrange the degrees of freedom which in the TTN case accumulate over successive coarse graining steps. By doing this the issue is circumvented. Keeping the same notation as in the previous section:

$$u : \mathbb{V}_{s'_1} \otimes \mathbb{V}_{s'_2} \rightarrow \mathbb{V}_{s_1} \otimes \mathbb{V}_{s_2}, \quad (3.43)$$

$$uu^\dagger = u^\dagger u = \mathbb{I}^{\otimes 2}, \quad (3.44)$$

$$\begin{array}{|c|} \hline u \\ \hline \\ \hline u^\dagger \\ \hline \end{array} = \begin{array}{|c|} \hline \\ \hline \\ \hline \\ \hline \end{array}, \quad (3.45)$$

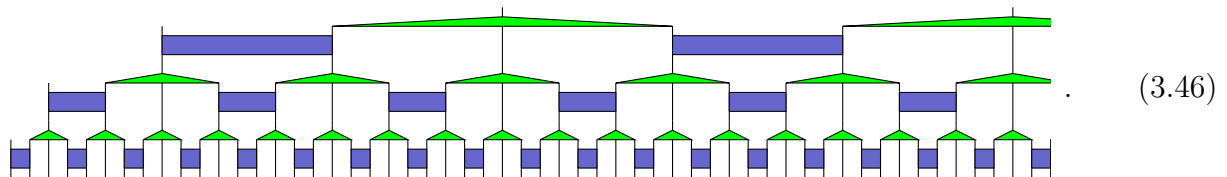
where $\mathbb{I}^{\otimes 2}$ is the identity on 2 sites as shown explicitly by the diagram.

Now a single renormalisation step⁴ is made up of two layers, first a row of disentanglers operate at the boundaries between blocks. Following this intermediate disentangling step a row

³ α here is a model dependent constant which grows with ξ .

⁴This is what is meant by entanglement renormalisation, a state after entanglement renormalisation has been applied produces a MERA network.

of isometries are applied to the resulting rearranged lattice sites thereby giving a renormalised lattice. This procedure is repeated until the resultant lattice yields a product state. Throughout the following discussion a layer or step of the MERA will refer to the combination of one row of disentanglers *and* a row of isometries. It should be noted that the disentangling operators do not leave individual blocks unentangled from the rest of the lattice, rather the entanglement localised at the boundary is discarded such that long range correlations are preserved thereby allowing for a well-defined renormalisation scheme. This defines the process of entanglement renormalisation. One can show that with the disentanglers that the MERA reproduces the logarithmic correction to the entanglement entropy for a 1D system and indeed also exhibits an area law for higher dimensional systems. Another important feature of the MERA is that correlations decay algebraically making the MERA a natural ansatz for critical states in 1D. The following diagram exemplifies the difference between real space renormalisation and MERA:



From a numerical point of view it has been found that the expectation values of local observables may be computed efficiently, for example 2 site operators or 2 point correlation functions. The efficiency of determining these values comes from the building blocks of the network. In order to evaluate an expectation value in this context one must contract the operator in question between two copies of the MERA. As a result many of the contractions are simply unitaries or isometries contracted with their conjugates which by definition of the tensors yield identity operators. In the end the contraction that is to be made is simplified greatly and the relevant tensors that are contracted will be contained within the causal cone of the operator. A defining property of the MERA is that the causal cone has a bounded width⁵. Essentially this means that at each layer of coarse graining only a few tensors lie within the causal cone of the operator, by few we mean $\sim \mathcal{O}(1)$. One can see this clearly in the accompanying figure.

As in the case of MPS and TTN the unitary tensors and isometric tensors need not be the same for each layer or even each site. However, for the same reasons as before they will be the same. We will look at translation invariant systems and in 1D in particular we will want to examine critical points, that is scale invariant states. In these cases the tensors will be restricted to being the same per site and per layer [42]. Indeed, this homogeneity of the network is a key property of the interpretation of the MERA network as a discrete realisation of AdS space which leads to the proposed AdS/MERA correspondence [6]. This will be discussed further in a later chapter.

At this point we exemplify the tensors which make up the MERA, we begin with an example of an isometry. Taking a binary scheme in this instance suppose we wish to coarse-grain a system of 4 spin- $\frac{1}{2}$ particles arranged in a chain and denoted by $[e_1 s_1 s_2 e_2]$. The aim of the coarse graining will be to reduce the two middle spins into an effective site s' . Taking the state of the system in the usual notation to be:

$$|\psi\rangle = \frac{1}{3} \left(2 |1001\rangle + \sqrt{2} |0110\rangle - \sqrt{2} |1100\rangle + |0100\rangle \right). \quad (3.47)$$

The procedure then to find the values of the components of w is to first determine the reduced

⁵One may take only this property as the definition of the ansatz. [40]

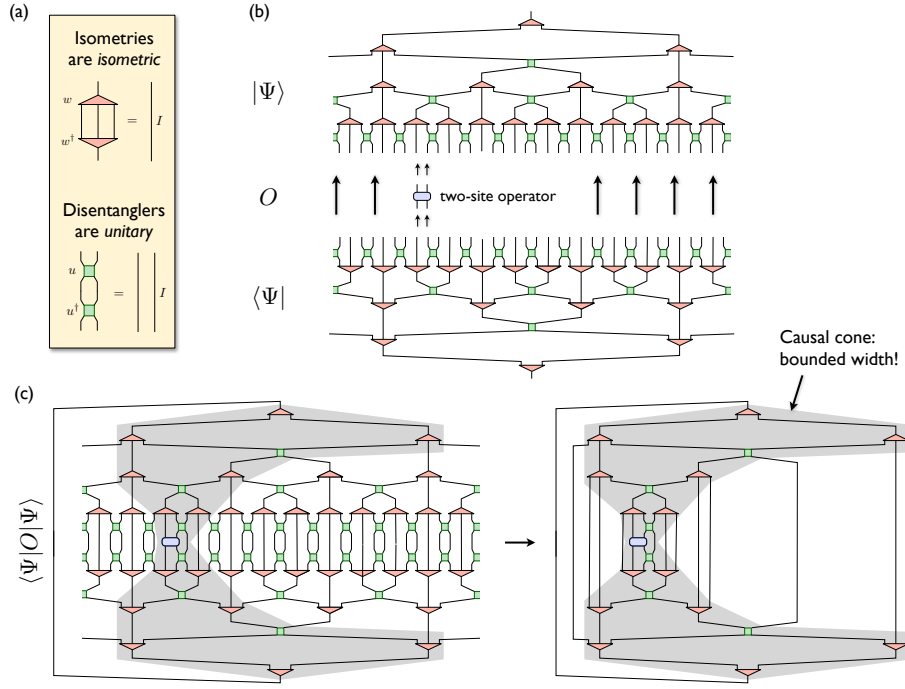


Figure 3.1: A ternary MERA network. (a) Isometric and unitary tensors when contract with their conjugates yield identities. (b) The process of determining an expectation value for some 2-site operator (c) The simplification of the contractions by using the properties of the tensors and the causal cone's bounded width. Figure originally appears in [41], we thank the author for permission to reuse this figure.

density matrix of the subsystem $[s_1, s_2]$ and write it in diagonal form:

$$\rho^{[s_1, s_2]} = \text{Tr}_{[e_1, e_2]} [\rho^{[e_1, s_1, s_2, e_2]}] = \sum_{i=0}^3 p_i |\rho_i\rangle \langle \rho_i|, \quad (3.48)$$

where $p_0 = p_1 = \frac{4}{9}$, $p_2 = \frac{1}{9}$, $p_3 = 0$ with eigenvectors:

$$\begin{aligned} |\rho_0\rangle &= \frac{2}{\sqrt{6}} |10\rangle + \frac{1}{\sqrt{3}} |11\rangle, & |\rho_1\rangle &= |00\rangle, \\ |\rho_2\rangle &= -\frac{1}{\sqrt{3}} |10\rangle + \frac{2}{\sqrt{6}} |11\rangle, & |\rho_3\rangle &= |01\rangle. \end{aligned} \quad (3.49)$$

Since one of the eigenvalues is zero the exact coarse graining can be achieved using a bond dimension of 3 rather than 4, without losing any information of the state. Moreover, we can find an approximate coarse graining by neglecting the next smallest eigenvalue. In that case the entries of w with effective site dimension $\chi = 2$ are:

$$w_{10}^0 = \frac{2}{\sqrt{6}}, \quad w_{11}^0 = \frac{1}{\sqrt{3}}, \quad w_{00}^1 = 1. \quad (3.50)$$

To retain the full information one needs the additional entries:

$$w_{10}^2 = -\frac{1}{\sqrt{3}}, \quad w_{11}^2 = \frac{2}{\sqrt{6}}. \quad (3.51)$$

We express the new coarse grained state as:

$$|\psi'_\chi\rangle = \sum_{k_1, k_3=0}^1 \sum_{k_2}^{\chi-1} \psi'_{k_1 k_2 k_3} |k_1 k_2 k_3\rangle, \quad (3.52)$$

where

$$\psi'_{k_1 k_2 k_3} = \sum_{k_1, k_2=0}^1 w_{k_1 k_2}^{i_2} \psi_{i_1 k_1 k_2 i_3}. \quad (3.53)$$

Explicitly this then yields the following effective state:

$$|\psi'_{\chi=2}\rangle = \frac{4}{3\sqrt{6}} |000\rangle - \frac{2}{3\sqrt{3}} |100\rangle + \frac{2}{3} |111\rangle, \quad (3.54)$$

$$|\psi'_{\chi=3}\rangle = \frac{4}{3\sqrt{6}} |000\rangle - \frac{2}{3\sqrt{3}} |100\rangle + \frac{2}{3} |111\rangle + \frac{1}{3\sqrt{3}} |020\rangle + \frac{2}{3\sqrt{6}} |120\rangle. \quad (3.55)$$

As an example of these disentangling tensors [43] we can consider the state of four spin- $\frac{1}{2}$ particles on a chain with an isometry w which coarse grains the middle two sites. Denoting the sites by $r_1 s_1 s_2 r_2$ we can say that the whole state is:

$$|\psi\rangle = \frac{1}{2} (|0\rangle_{r_1} |1\rangle_{s_1} + |1\rangle_{r_1} |0\rangle_{s_1}) (|0\rangle_{r_2} |1\rangle_{s_2} + |1\rangle_{r_2} |0\rangle_{s_2}) \quad (3.56)$$

$$= \frac{1}{2} (|0101\rangle + |0110\rangle + |1001\rangle + |1010\rangle). \quad (3.57)$$

Evidently the spins r and s are pairwise maximally entangled in Bell states as can be seen also from the reduced density matrix:

$$\rho_{s_1 s_2} = Tr_{r_1 r_2} \rho = Tr_{r_1 r_2} |\psi\rangle \langle \psi| \quad (3.58)$$

$$= \frac{1}{4} (|00\rangle \langle 00| + |01\rangle \langle 01| + |10\rangle \langle 10| + |11\rangle \langle 11|). \quad (3.59)$$

Simply coarse graining this state will either result in unacceptable errors from truncating the bond dimension or force us to keep the full state space. To alleviate this issue we introduce disentanglers operating on the pairs $r_1 s_1$ and $s_2 r_2$ defined as:

$$u = \sum_{i,j,a,b=0}^1 u_{ij}^{ab} |a\rangle_r |b\rangle_s \langle i|_r \langle j|_s, \quad (3.60)$$

where the only non-zero elements are:

$$u_{01}^{00} = u_{10}^{00} = u_{01}^{01} = -u_{10}^{01} = \frac{1}{\sqrt{2}}, \quad (3.61)$$

$$u_{00}^{10} = u_{11}^{11} = 1. \quad (3.62)$$

This unitary tensor effectively maps the Bell state to a state in the standard computational basis, i.e.

$$u : \frac{1}{\sqrt{2}} (|0\rangle |1\rangle + |1\rangle |0\rangle) \mapsto |00\rangle. \quad (3.63)$$

So the state of four spins is mapped to $|0000\rangle$ which causes no issues under coarse-graining, the reduced density matrix is simply:

$$\rho_{s_1 s_2} = |00\rangle \langle 00|. \quad (3.64)$$

As already hinted at the disentangling operation can be seen as a change of basis as above or as a reversible reorganisation of degrees of freedom as a preparation for the coarse-graining transformation.

So far we have only given an overview of the MERA scheme, if one wishes to make further reading on numerical results and determining ground states using this ansatz then the works of Evenbly and Vidal [27, 31, 39, 44, 45] contain a great many benchmark results.

3.4.1 MERA Examples

To solidify the structure of MERA in one's mind some examples are useful at this point. We will take the same states as before to see the difference in MPS and MERA representations.

GHZ State

If we choose as the state $(|0\rangle + |1\rangle)/\sqrt{2}$ as the top tensor of the MERA then using a ternary scheme we may obtain the $|GHZ\rangle$ by the choice:

$$u = \mathbb{I}, \quad w_l^{ijk} = \delta_l^{ijk}. \quad (3.65)$$

Given a little thought it should become clear that this will yield the required state. One may also notice that given the choice of unitary tensors this proposed scheme is in effect a TTN scheme since the disentglers act trivially.

W State

To recover the W state here we propose the following binary scheme:

$$u = \mathbb{I}, \quad w_0^{00} = w_1^{10} = w_1^{01} = 1. \quad (3.66)$$

Applying this scheme to a top tensor $T \equiv |1\rangle$ yields the W state, since this choice of top tensor can be seen as in effect the "trivial" W state. Applying the isometries above to any W state will yield another W state on double the number of sites.

3.4.2 Properties of the MERA

In this subsection we make note of a few more aspects of the MERA which will be relevant in the discussions which follow.

First we note that for a given initial finite lattice of N sites the MERA that arises from the entanglement renormalisation procedure has a *bounded depth*. That is, after finite number of renormalisation steps or layers the MERA produces a product state or terminates in a single tensor which in the literature is referred to as the *top tensor*. Another piece of nomenclature associated with MERA is the rank of a MERA network. This is the dimension of the dual index of the top tensor and is usually denoted by χ_T . It is equivalent to the dimension of the state space of the final effective site, given by the final "arm" of the top tensor. For χ_T a MERA represents a single pure state, usually the ground state. In this case strictly speaking there is no dual index the MERA terminates at the top tensor. This would mean that in the language of Penrose graphical tensor notation that the MERA is a rank($N, 0$) tensor network. For MERA rank greater than 1, this usually indicates a ground state degeneracy or represents the ground state and $\chi_T - 1$ lowest energy states. In this situation the MERA is a rank($N, 1$) network. Now, due to the exponential coarse graining of the original lattice the top tensor will be reached in $T = \log(N)$ steps/layers. The base of the log will depend on the coarse-graining scheme in question, usually 3-to-1 or 2-to-1.⁶ As for the numerical benefits, since the growth of the network is logarithmic the number of tensors needed to construct the network will be of order $\mathcal{O}(N)$ and as a result the memory required to store a MERA will be of order $\mathcal{O}(\chi^{\#legs} N)$ since the number of elements in each tensor is $\chi^{\#legs}$.

So far the view we have taken of the MERA network is as a variational ansatz, where the tensors themselves are the variational parameters. However, one may view the network in

⁶We refer to MERA networks incorporating these schemes as ternary and binary MERA respectively.

another manner. One may view the network as a quantum circuit and in fact in some situations this will be necessary. To view the network as such, a slight modification to the network but one which does not affect its physical properties. For a brief introduction to quantum circuits the reader should refer to the appendix, for an in depth and complete picture one should consult *Quantum Computation and Quantum Information* [17]. In the renormalisation viewpoint of MERA where the initial lattice is the starting point from which we evolve in some sense to an effective lattice and eventually to a top tensor or product state we are viewing the MERA from the bottom-up. In the quantum circuit view we "evolve" in the opposite manner, we begin with an initialised state say of N -qubits,

$$|\Psi_0\rangle = \underbrace{|00\dots 0\rangle}_N, \quad (3.67)$$

and the MERA is acts on this state giving the state which was the starting point of the entanglement renormalisation. This is in effect a top-down view of the MERA network. One should notice an issue with this viewpoint, previously we have stated that the MERA network is a rank($N, 0$) or rank($N, 1$) network. However, for an N -qubit state a quantum circuit acting on this state should be a unitary operator or equivalently a rank(N, N) network. As such we make the modification mentioned previously. We know that quantum computations do not destroy degrees of freedom, they simply modify qubits by flipping qubits or rearranging them and so on, whereas in the MERA we have coarse-graining operations which do destroy degrees of freedom. To reconcile this difference we must add more dual "legs"⁷ to make the MERA network, \mathcal{M} , a rank(N, N) network⁸. These additional "arms" are added to the isometries and to the top tensor such that the resultant network is made entirely of unitary operators⁹. The way that we do this is to give these tensors additional dual indices which are contracted with $|0\rangle$ input vectors. In this way the isometries w and top tensor t become unitary gates in the circuit. As an example we can see that the isometry w may be made of a unitary tensor v contracted with constant $|0\rangle$ vectors,

$$w = w_{\sigma}^{\alpha\beta\gamma} |\phi_{\alpha}\rangle |\phi_{\beta}\rangle |\phi_{\gamma}\rangle \langle\phi_{\sigma}| = v_{\sigma\rho\theta}^{\alpha\beta\gamma} |\phi_{\alpha}\rangle |\phi_{\beta}\rangle |\phi_{\gamma}\rangle \langle\phi_{\sigma}| \langle\phi_{\rho}|0\rangle \langle\phi_{\theta}|0\rangle, \quad (3.68)$$

where we have that:

$$w^{\dagger}w = \langle 0| \langle 0| v^{\dagger}v |0\rangle |0\rangle = \langle 0|0\rangle^2 \mathbb{I} = \mathbb{I}, \quad (3.69)$$

using the unitarity of v . With this modification we may view the MERA in a top-down fashion as a quantum circuit. With this viewpoint the isometric tensors add new degrees of freedom to the circuit and the disentanglers entangle these new degrees of freedom until in principle we have a state with entanglement at all length scales.

The notion of a past causal cone that was mentioned previously is more readily explained in this quantum circuit picture. Given a MERA circuit suppose that we wish to trace a computation of some site s on the final state/lattice \mathcal{L}_0 . By direct inspection of the network one can see that the number of wires and gates affecting the state is limited at all stages of the computation. In fact for a ternary MERA the past causal cone has a bounded width of 2 sites for a single site on a 1 dimensional lattice, this is true at all depths. The bounded width of the causal cone, \mathcal{C} , holds for arbitrary dimensions. To justify this consider a binary MERA and take a time slice of the causal cone, \mathcal{C} , at time τ . Suppose this time slice is formed by a (hyper)cube of h^d effective lattice sites, where h is the side length. By definition the disentangling operators

⁷"Arms" are equivalent to dual "legs", this is a mixing of the nomenclature of tensor indices and graphical notation.

⁸Remember that this is equivalently a unitary operator or a quantum circuit.

⁹These unitary operators/tensors are often referred to in this context as (quantum) gates, using the vocabulary of quantum information.

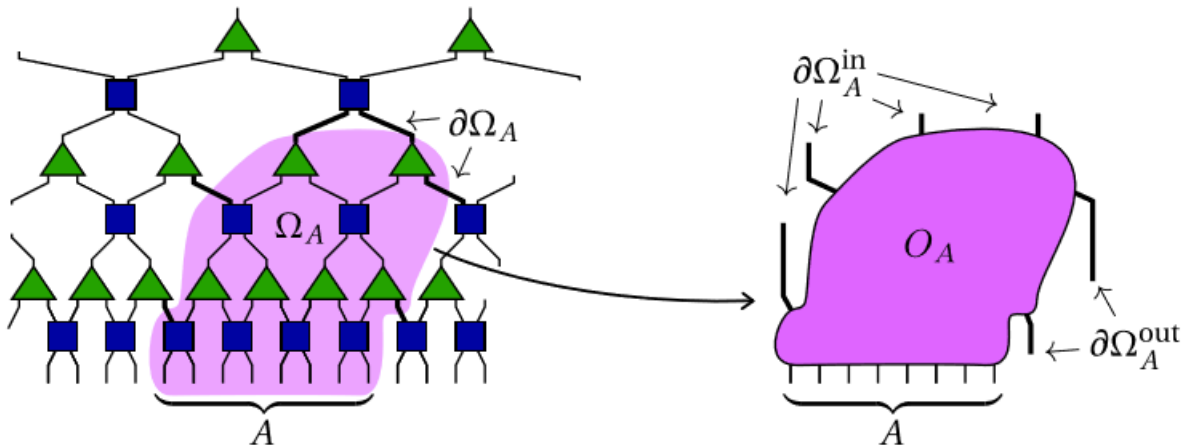


Figure 3.2: Left: An example MERA with a subsystem A . Right: The relevant bonds from an arbitrary region encompassing A . Figure originally from [46]

act only locally so as a worst case scenario, moving back up the network, they may expand the causal cone by one lattice site in all directions. This gives after entangling a (hyper)cube of $(h+2)^d$ sites. Next the coarse-graining step is performed which for a binary MERA will take block of 2^d sites to one site. The worst case scenario here will be if the coarse-graining block only intersects \mathcal{C} at a single site at the corner of the (hyper)cube. As a result each edge of the $(h+2)^d$ cube is reduced to $(h+1)$ sites which must be split into 2, leaving a possible remainder. As such the (hyper)cube is divided into:

$$\left(\left\lceil \frac{h+1}{2} \right\rceil + 1 \right)^d \quad (3.70)$$

blocks, with the 1 coming from the lone corner site. This expression gives us the number of effective site on the $\tau+1$ lattice, $\mathcal{L}_{\tau+1}$. We should find that this evaluates to less than or equal to h^d for the \mathcal{C} to shrink or reach a bounded width, though it may grow before this point. It is readily verified that for $h < 3$ the cube size grows until settling on a value of $h = 3$. If $h > 4$, the cube shrinks until reaching a size of $h = 4$. Since we the analysis was for a worst can the causal cone can fluctuate but should never exceed $h = 3$ coming from below.

With all of these properties noted we can demonstrate the bound on entanglement entropy for a MERA.

3.4.3 EE Bound for MERA

Now we present the behaviour of the Entanglement Entropy in a MERA tensor network. [46] We find remarkably that in fact the area law proposed by Ryu-Takayanagi emerges in MERA represented states. We will present a proof/argument given initially by Hauru which generalises to arbitrary dimensional MERA. However the argument is most understandable for a 1 dimensional state as we can use the language of Quantum Circuits in a reasonably straight forward manner. One should refer to the Appendix for a primer on quantum circuits.

Our objective here is to determine a bound on the entropy \mathcal{S}_A for $A \subset \mathcal{L}$. To begin we take an arbitrary subset of the MERA network which contains the UV sites in A and we will denote this by $\Omega_A \in M$ where M is the total network.

Now consider all the bonds crossing the boundary of Ω_A , denoted by $\partial\Omega_A$ ¹⁰. The initial

¹⁰The physical legs won't be included in the boundary.

argument will be to show that:

$$\mathcal{S}_A \leq \sum_{s \in \partial\Omega_A} S_s, \quad (3.71)$$

where S_s is the measure of single site entanglement i.e. the EE of each bond s w.r.t. the rest of the effective lattice. One can think of this as the measure of EE if one bond s is cut and the rest of the lattice is traced out from the density matrix, ρ_s . In MPS states this is the strength of the bonds between matrices in the MPS.

A couple of notes to make before continuing. Unitary transformations leave entropy unchanged. In particular a disentangling gate/tensor will leave the eigenvalues of an input state/density matrix unchanged. So, $\mathcal{S}_{\rho^{in}} = \mathcal{S}_{\rho^{out}}$. Then viewing the MERA network in the quantum circuit interpretation we will have both disentangling and coarse-graining/isometric tensors in the network as unitary gates. Thus for all MERA tensors $\mathcal{S}^{in} = \mathcal{S}^{out}$.

Now we split the boundary, $\partial\Omega_A$, into two sets of bonds $\partial\Omega_A^{in}$ and $\partial\Omega_A^{out}$, see figure. Moreover, we consider Ω_A as a single entropy preserving isometry as it is composed of unitary MERA tensors which may be contracted to form a single operator, \mathcal{O}_A .

$$\partial\Omega_A \xrightarrow[\text{inner tensors}]{\text{contract}} \mathcal{O}_A = (\mathcal{O}_A)_{\alpha_1\alpha_2}^{\beta_1\beta_2\beta_3\beta_4}. \quad (3.72)$$

Now we recall the triangle/Araki-Lieb inequality¹¹:

$$|\mathcal{S}(\rho_A) - \mathcal{S}(\rho_B)| \leq \mathcal{S}(\rho) \leq \mathcal{S}(\rho_A) + \mathcal{S}(\rho_{A^c}), \quad (3.73)$$

where the second inequality stems from sub-additivity.

Now using this relation and that \mathcal{O}_A preserves entropy we find, taking $\mathcal{S}(\rho_X) = \mathcal{S}_X$:

$$\begin{aligned} \mathcal{S}_A - \mathcal{S}_{\partial\Omega_A^{out}} &\leq \left| \mathcal{S}_A - \mathcal{S}_{\partial\Omega_A^{out}} \right| \leq \mathcal{S}_{A \cup \partial\Omega_A^{out}} = \mathcal{S}_{\partial\Omega_A^{in}}, \\ \implies \mathcal{S}_A &\leq \mathcal{S}_{\partial\Omega_A^{out}} + \mathcal{S}_{\partial\Omega_A^{in}} \leq \sum_{s \in \partial\Omega_A^{in}} S_s + \sum_{s \in \partial\Omega_A^{out}} S_s = \sum_{s \in \partial\Omega_A} S_s. \quad \blacksquare \end{aligned}$$

Now we note that Ω_A may be chosen to be minimal in the sense that the boundary, $\partial\Omega_A$, gives the tightest possible bound on \mathcal{S}_A . This will be the bound for the scaling of the entanglement entropy as A grows. For this we will look at the binary MERA network for clarity of discussion but the argument holds more generally.

Recall that for a Hilbert space of dimension χ the maximal EE is given by $\log_2(\chi)$ i.e. the maximally mixed state. Then for each bond $s \in \partial\Omega_A$ we have the bound $\mathcal{S}_s \leq \log_2(\chi)$. Hence,

$$\mathcal{S}_A \leq |\partial\Omega_A| \log_2(\chi). \quad (3.74)$$

So the question becomes a matter of determining $\partial\Omega_A$ which in effect is the number of bonds puncturing the boundary of the region. We begin by making the choice of $\Omega_A = \mathcal{C}_A$, that is, to be the causal cone of the subsystem A . We mean here the causal cone in the MERA sense. [(This needs a reference)]. The key property here of the causal cone is that for some d -dimensional region A of size l^d the causal cone \mathcal{C}_A will shrink with each layer of the MERA until it reaches a size of 4^d . This will occur after $\mathcal{O}(\log_2(l))$ layers of the MERA since at that point the region A will have been reduced to a single site and the causal cone starts to resemble the a 1-site causal cone. Again this is for a binary MERA and can be checked by inspection of the network.

For the $d=1$ case, \mathcal{C}_A has 2 wires/bonds at each layer to that the number of wires crossing the boundary is:

$$|\partial\mathcal{C}_A| \approx 4 + 2 \log_2(l),$$

¹¹B here denotes some other splitting of the system.

$$\implies \mathcal{S}_A \leq |\partial\mathcal{C}_A| \log_2(\chi) \sim \mathcal{O}(\log_2(l)).$$

So we've recovered the $\log(l)$ scaling of EE in 1D.

For $d > 1$ we have: \mathcal{C}_A at layer τ consists of the order of $\left(\frac{l}{2^\tau}\right)^{d-1}$ wires crossing the boundary. This gives the following:

$$\begin{aligned} |\partial\mathcal{C}_A| &\approx 4^d + \sum_{\tau=1}^{\log_2(l)} \left(\frac{l}{2^\tau}\right)^{d-1}, \\ &= 4^d + l^{d-1} \left[\frac{(2^{d-1})^{\log_2(l)} - 1}{(2^{d-1})^{\log_2(l)}(2^{d-1} - 1)} \right], \\ &= 4^d + l^{d-1} \left[\frac{l^{d-1} - 1}{l^{d-1}(2^{d-1} - 1)} \right], \\ &= 4^d + \frac{l^{d-1} - 1}{2^{d-1} - 1}, \end{aligned}$$

$$\implies \mathcal{S}_A \leq |\partial\mathcal{C}_A| \log_2(\chi) \sim \mathcal{O}(l^{d-1}), \quad (3.75)$$

so evidently the MERA network ansatz reproduces area law behaviour of entanglement entropy. This bound is usually saturated for the case of scale-invariant MERA.

Chapter 4

AdS/MERA

In this chapter we present the interpretation first proposed by Swingle [6, 32] of the MERA tensor network as a discretization of Anti-de Sitter spacetime. In this context the MERA that is referred to is a scale invariant network of a 1 dimensional lattice and hence represents the critical point of the associated lattice field theory. At the critical point the field theory flows to a conformal field theory in the renormalisation group sense. As such the MERA becomes analogous to the CFT. However in addition from the structure of the network Swingle proposed the interpretation of the tensor network itself as a bulk geometry similar to an Anti-de Sitter space time, Fig.(4.1). Since this proposal several other advances have been made, namely a continuous version of the MERA network has been proposed [47]. This so called cMERA will be the focus of the following chapter where we will describe the framework in some detail and present several results obtained by these methods for bosonic and fermionic theories [8].

For the purpose of this discussion one should have some familiarity with the basics of the AdS/CFT correspondence. At this point in time there are many sources to refer to [49–51] and accessible lectures [52] but for the moment it should be sufficient to know that the AdS/CFT correspondence¹ is a proposal that certain quantum field theories which do not include gravity are in fact dual to a gravitational theory in a higher dimensional curved “bulk” geometry. In other words, d -dimensional QFT \leftrightarrow $(d + 1)$ -dimensional bulk gravity theory. We will present several results from holography in what follows, it will be made clear when this occurs.

Shortly after the initial proposal of a holographic correspondence it was seen that real space renormalisation was important to the framework. [53] With the advent of entanglement renormalisation it could be suggest that combining these two theories would be a promising direction to explore. As usual we denote a subregion of our many-body quantum system by A , which will be of linear size L . The degrees of freedom of the system will be partitioned into groups/blocks spaced in $\log(r)$ with a measure of dr/r where r is the length scale of study. As mentioned previously we expect that the measure of entropy from A at scale r will be proportional to the size of the boundary ∂A in units of the coarse-grained scale r . Infinitesimally we have that

$$d\mathcal{S}(r) \sim \left(\frac{L}{r}\right)^{d-1} \frac{dr}{r}. \quad (4.1)$$

Then to determine the entanglement entropy one integrates this expression from the ultraviolet (UV) cut-off to the larger infrared (IR) cutoff which will either be to the point where the system has been renormalised to be a product state or to a single point. In the MERA picture this would be from the scale of the original lattice or the UV theory up to the top tensor where the state has either been factorised or the MERA terminates at the top tensor, this would be the IR theory. In the holographic picture this IR length is $\min(L, \xi_E)$ where ξ_E is the length

¹Also referred to as holography or the gauge/gravity correspondence.

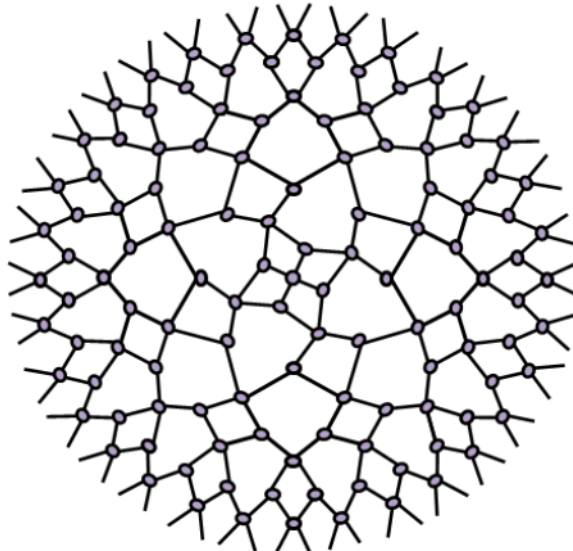


Figure 4.1: A visualisation of a periodic MERA as a discrete AdS space. Figure from [48].

scale beyond which there is no entanglement. For $d > 1$ the result of this integral reproduces an area/boundary law,

$$\mathcal{S}_{d>1} \sim \left(\frac{L}{\epsilon}\right)^{d-1} - \left(\frac{L}{\min(L, \xi_E)}\right)^{d-1}, \quad (4.2)$$

and the logarithmic correction for $d = 1$,

$$\mathcal{S}_{d=1} \sim \log\left(\frac{\min(L, \xi_E)}{\epsilon}\right), \quad (4.3)$$

where ϵ is a UV cut-off to prevent the integral diverging.

Looking now towards the lattice, as mentioned the UV theory is associated with the original lattice and after the entanglement renormalisation procedure we obtain the IR theory. In between at each layer of the MERA² we have an effective lattice at an effective length scale. As before we label the layer by $\tau = 0, 1, 2, \dots$, and the lattice spacing by a such that the different length scales are related by:

$$\log\left(\frac{r_\tau}{a}\right) = \tau \log(2), \quad (4.4)$$

such that $\tau = 0$ corresponds to the original lattice length scale $r_0 = a$. While in the quantum circuit viewpoint $-\tau$ is taken to be "computation time" here we view τ as parametrizing the depth of an emergent dimension representing the renormalisation group scale. Then each site in the network is viewed as a cell filling a higher dimensional "bulk" geometry. This defines a discrete geometry from the network itself and is in effective the insight put forward by Swingle. It should be emphasised that in the subsequent calculations of entanglement entropy in this framework that only tensor within the causal cone of a region A of the boundary will contribute to the calculation as we argued in the calculation of the entropy bound for MERA. Moreover the boundary of the causal cone is a minimal curve in the bulk geometry as it represents the minimal number of sites which need to be traced out in calculating the reduced density matrix of the region. Moreover numerically it has been shown that the entanglement entropy is proportional to this minimal curve [54].

The claim then is that the discrete geometry that is produced by the network is in fact a

²The MERA in this case is a binary MERA.

discrete Anti-de Sitter (AdS) space. The metric for smooth AdS in 2-dimensions is given by:

$$ds^2 = R^2 \left(\frac{dr^2 + dx^2}{r^2} \right) = R^2 \left(dw^2 + \frac{\exp(-2w)}{a^2} dx^2 \right), \quad (4.5)$$

where R is a constant³ and $w = \log(r/a)$ where a is a cut-off for small r . A larger R corresponds to a larger geometry and hence more entanglement since in the MERA picture a larger depth would correspond to more layers as a result of the initial state being more entangled. Then in the context of the lattice model R is linked to the strength of the disentanglers and hence the entropy of local sites. In the holographic context R has been found to be proportional to the central charge c at critical points. In order to make this connection between AdS and MERA we can examine the length of two curves in either geometry, this is the comparison made by Swingle.

The curves we take, γ_1 and γ_2 , are parametrized by:

$$\gamma_1 = \{x(t) = x_0 t, r(t) = r_0 | t \in [0, 1]\} \quad (4.6)$$

$$\gamma_2 = \{x(t) = x_0 \cos(\pi t), r(t) = x_0 \sin(\pi t) | t \in [0, 1]\}. \quad (4.7)$$

In the AdS geometry γ_1 is a line at fixed depth r_0 while γ_2 is a geodesic connecting $(x_0, 0)$ to $(-x_0, 0)$. To calculate the length of these curves we calculate directly from the formula for the length of a parametrized curve:

$$|\gamma| = \int_0^1 dt \sqrt{g_{\mu\nu} \dot{\gamma}^\mu \dot{\gamma}^\nu}, \quad (4.8)$$

where $g_{\mu\nu}$ is the AdS metric described above. The first calculation is straightforward:

$$\begin{aligned} |\gamma_1| &= \int_0^1 dt \sqrt{g_{\mu\nu} \dot{\gamma}^\mu \dot{\gamma}^\nu}, \\ &= \int_0^1 dt \sqrt{g_{xx} \dot{\gamma}^x \dot{\gamma}^x}, \\ &= \int_0^1 dt \sqrt{\frac{R^2}{r^2(t)} \dot{x}^2(t)}, \\ &= \int_0^1 dt \sqrt{\frac{R^2}{r_0^2} x_0^2}, \\ &= R \frac{x_0}{r_0}. \end{aligned} \quad (4.9)$$

For the second curve we need to be more careful since in AdS geodesics are of infinite length so we need to impose a cut-off for small r .

$$\begin{aligned} |\gamma_2| &= \int_0^1 dt \sqrt{g_{\mu\nu} \dot{\gamma}^\mu \dot{\gamma}^\nu}, \\ &= \int_0^1 dt \sqrt{g_{xx} \dot{\gamma}^x \dot{\gamma}^x + g_{rr} \dot{\gamma}^r \dot{\gamma}^r}, \\ &= 2 \int_0^{\frac{1}{2}} dt \sqrt{\frac{R^2}{r^2(t)} (-x_0 \pi \sin(\pi t))^2 + \frac{R^2}{r^2(t)} (x_0 \pi \cos(\pi t))^2}, \\ &= 2 \int_0^{\frac{1}{2}} dt \sqrt{\frac{R^2 x_0^2 \pi^2}{x_0^2 \sin^2(\pi t)} (\sin^2(\pi t) + \cos^2(\pi t))}, \end{aligned}$$

³Usually this is referred to as the AdS radius.

$$|\gamma_2| = 2\pi R \int_0^{\frac{1}{2}} dt \frac{1}{\sin(\pi t)}, \quad (4.10)$$

where we've taken the limits from 0 to 1/2 since the integral is symmetric. Next we use the standard solution to this integral to find:

$$|\gamma_2| = \frac{2\pi R}{\pi} \left[-\log \left(\cos \left(\frac{\pi t}{2} \right) + \sin \left(\frac{\pi t}{2} \right) \right) \right]_{t=0}^{t=\frac{1}{2}}. \quad (4.11)$$

The upper limit yields zero since $\sin(\pi/4) = \cos(\pi/4)$ and we note that $\log(\cos(0)) = 0$ so in fact the only term of consequence comes from the lower limit which is $\log(\sin(\pi t/2)) \rightarrow \infty$ as $t \rightarrow 0$. It is at this point that a cut-off becomes necessary to regularise this infinity. To do this suppose we shift the lower limit to a non-zero value $\alpha \ll 1$. Then the integral evaluates to:

$$|\gamma_2| = -2R \log \left(\sin \left(\frac{\pi \alpha}{2} \right) \right). \quad (4.12)$$

Now we use that for small $x \ll 1$ $\sin(x) \approx x$ we have that:

$$|\gamma_2| = -2R \log \left(\frac{\pi \alpha}{2} \right). \quad (4.13)$$

So the question at this point is: what is α ? We know that α is small and hence close to the boundary of the space so it should characterise r close to the boundary, that is, $r(t) \approx x_0 \pi t$ using the small angle approximation. Moreover, the UV cut-off of r for the field theory is ε . Thus, $\alpha = \frac{\varepsilon}{x_0 \pi}$. As a result we find that:

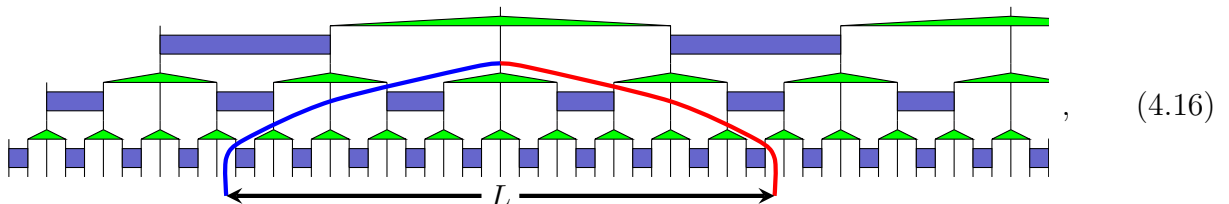
$$\begin{aligned} |\gamma_2| &= -2R \log \left(\frac{\pi}{2} \frac{\varepsilon}{x_0 \pi} \right), \\ &= 2R \log \left(\frac{2x_0}{\varepsilon} \right), \\ &= 2R \log \left(\frac{x_0}{a} \right), \end{aligned} \quad (4.14)$$

taking $a = \varepsilon/2$. Now we compare to similar curves through the discrete version of AdS, that is the MERA network. The first curve will again be the straight line distance at fixed depth. Using that R is the strength of a bond in the network, or equivalently the length per bond, we have that the length of the curve in units of x_0/a at the lattice scale, $r = a$, is $R(x_0/a)$. Then the corresponding length at RG step w_0 is given by:

$$|\gamma_1| = R \left(\frac{x_0}{a} \right) e^{-w_0} = R \left(\frac{x_0}{r_0} \right), \quad (4.15)$$

which agrees with the continuous result.

The lattice analogue of the geodesic curve is slightly more subtle. At the lattice scale suppose we have again two points separated by a lattice distance x_0/a . Then the minimal path through the lattice connecting these points will be made up essentially of two paths, beginning at the start and end point on the original lattice which extend into the network until they meet at a depth where the renormalisation brings them together. The figure below shows the concept more clearly:



As we know, any section of a lattice of size L will be coarse grained to a point in $\log(L)$ steps by the MERA. Again taking R to be the length per bond we have that at a depth $\log(x_0/a)$ the two paths meet. Therefore the total length of the discrete geodesic will be:

$$|\gamma_2| = 2R \log\left(\frac{x_0}{a}\right). \quad (4.17)$$

This result then agrees with the continuous case.⁴ This result is the first evidence of an AdS/MERA correspondence.

4.1 cMERA

At this point we would introduce the ideas involved in bringing MERA into the continuum. This section follows closely the presentation of the introductory work [47] and the subsequent work which is relevant to the following chapter [8].

In some sense it becomes natural to ask if we can apply MERA techniques to a quantum field theory. In physics there is often the issue of dealing with many degrees of freedom, whether in many-body physics or in relativistic QFT. In order to gain some insight into a problem renormalisation group techniques are employed to examine the problem at an appropriate length scale. In the original formulation RG methods are applicable to quantum systems using the quantum-to-classical mapping, which may fail in some cases. From this beginning Wilson's numerical renormalisation can be seen as an implementation of RG methods at the level of the wave function.

The difference between the Wilson RG scheme and entanglement renormalisation (MERA, tensor network methods) is that Wilson's RG scheme is a fixed scheme while TN methods are in general a variable RG scheme where the variational parameters are the tensors themselves [33]. While other tensor networks are similar in this regard it is the support for algebraically decaying correlations and the agreement with entropy and area law results from holography in $(1+1)$ -dimensions that sets MERA apart from say tree tensor networks or matrix product states.

Before introducing continuous MERA methods it should be made clear which view of the MERA we are taking. We take the quantum circuit viewpoint. In this context the MERA is understood in a top-down manner. Starting from a simple fiducial state, $|\mathbf{0}\rangle = |0\rangle^{\otimes N}$ for example, of quantum spins the state is acted upon by a unitary operator:

$$U_1 = \bigotimes_{j=1}^{N/2} u_j, \quad (4.18)$$

which entangles adjacent sites. This is followed by a scale transformation and renormalisation so that the lattice spacing and number of spins are unchanged. We denote this step by \mathcal{R} . It is equivalent to the coarse-graining step we saw before but modified for the quantum circuit picture. If the depth of the MERA is $\tau = T = \log(N)$ then the output of the circuit is the MERA state:

$$|\Psi_{MERA}\rangle = U_T \mathcal{R} U_{T-1} \mathcal{R} \dots \mathcal{R} U_1 |\mathbf{0}\rangle. \quad (4.19)$$

The question at this point is how to translate the scale transformation, (dis)entangling operation and fiducial state to continuum analogues. We may first assume that we have some quantum field theory with a given Hamiltonian. It will be necessary to enforce an ultra-violet cut-off for the QFT, which will be denoted by:

$$\text{Ultraviolet Cut-off: } \Lambda = \frac{1}{a}, \quad (4.20)$$

⁴Strictly speaking there will be other contributions to the discrete length that we've neglected to mention but these will be $\mathcal{O}(1)$ so will be entirely dominated by the logarithm.

where as before a is the lattice constant. The Hilbert space defined by the fields with such a cut-off will be denoted by \mathcal{H}_Λ such that:

$$|\Psi(u)\rangle \in \mathcal{H}_\Lambda, \quad (4.21)$$

where u parametrizes the fields and represents the length scale of interest. This parameter is taken such that the momentum k will be effectively cut-off as $|k| \leq \Lambda \exp(u)$. In connection to the discrete case, u effectively corresponds to the layer index τ . By reason of convention we have that u runs over $[-\infty, 0]$, such that the UV and IR limits are given by:

$$u = u_{UV} = 0, \quad u = u_{IR} \rightarrow -\infty. \quad (4.22)$$

The states given at these limits are defined as:

$$\begin{aligned} |\Psi(u_{IR})\rangle &\equiv |\Omega\rangle, & \text{Factorised reference state (unentangled),} \\ |\Psi(u_{UV})\rangle &\equiv |\Psi\rangle, & \text{Ground state of Hamiltonian (typically).} \end{aligned} \quad (4.23)$$

Importantly the IR state $|\Omega\rangle$ is also defined by the fields as:

$$\left(\sqrt{M}\phi(x) + \frac{i}{\sqrt{M}}\pi(x) \right) |\Omega\rangle = 0, \quad (4.24)$$

$$M^2 = \Lambda^2 + m^2, \quad (4.25)$$

with the properties:

$$\langle \Omega | \phi(k)\phi(k') | \Omega \rangle = \frac{1}{2M}\delta^d(k+k'), \quad \langle \Omega | \pi(k)\pi(k') | \Omega \rangle = \frac{M}{2}\delta^d(k+k'). \quad (4.26)$$

If the IR state were chosen as the vacuum state then the resultant cMERA state $|\Psi\rangle$ only contains particles with momenta below the UV cut-off Λ [47]. Moreover the IR state (4.24) is unentangled since the entanglement entropy S_A is vanishing for a subsystem A because all modes for any x are decoupled from one another.

Now, as in the lattice implementation we can relate a state at any layer or length scale of the MERA to the reference state by a unitary transformation as follows:

$$|\Psi(u)\rangle = U(u, u_{IR}) |\Omega\rangle, \quad (4.27)$$

or similarly the in terms of the UV state as:

$$|\Psi\rangle = U(0, u) |\Psi(u)\rangle. \quad (4.28)$$

Likewise an operator, \mathcal{O} , can be defined at any cMERA scale u as:

$$\mathcal{O}(u) \equiv U(0, u)^{-1} \cdot \mathcal{O} \cdot U(0, u), \quad (4.29)$$

which will be particularly useful in defining the Hamiltonian at different scales.

The form of this unitary operator that is presented in the literature [8, 47] is:

$$U(u_1, u_2) = \mathcal{P} \exp \left[-i \int_{u_2}^{u_1} K(u) + L du \right]. \quad (4.30)$$

Evidently this expression calls for explanation. Firstly, $K(u)$ and L are the continuum analogues of the disentangling and coarse-graining transformations respectively. \mathcal{P} denotes a path ordering

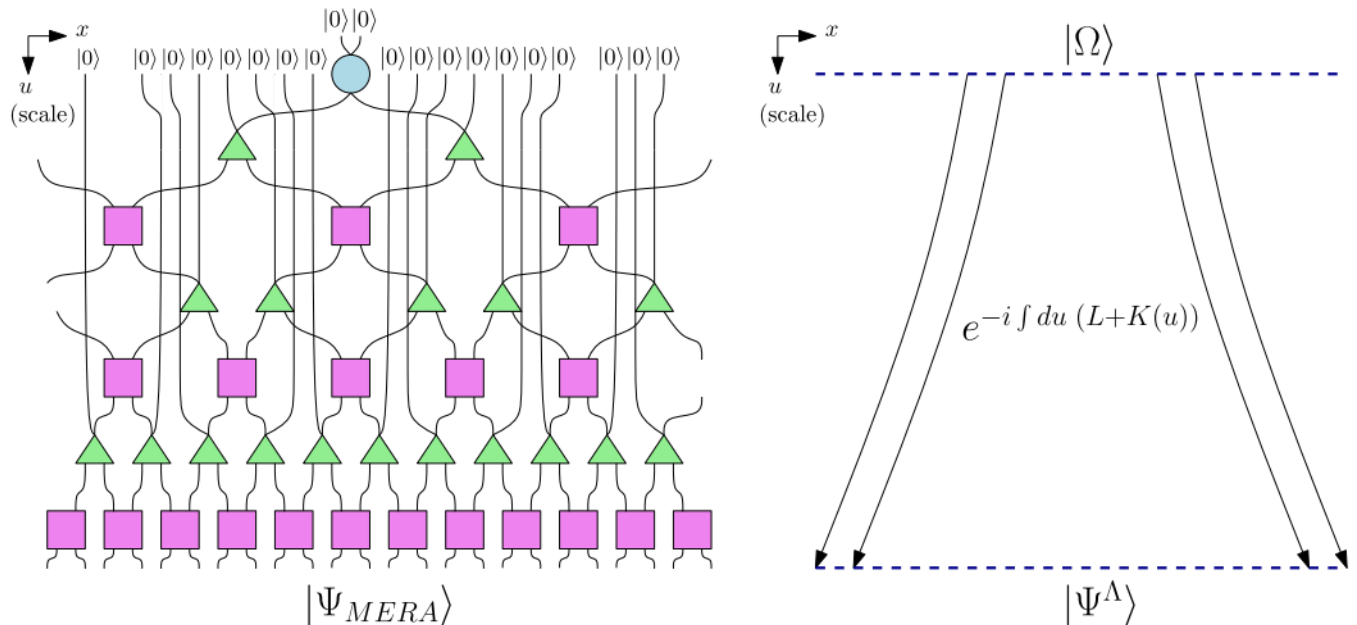


Figure 4.2: Left: The MERA viewed as a quantum circuit. Right: A similar schematic view of the cMERA. Figure from [23].

such that operators are ordered from large to small values of u .⁵ Some comments on these operators. The scale transformation acting on the IR state leaves it invariant since by definition the IR state is unentangled so each spatial point is independent from any other point. The entangling operator, $K(u)$, is designed to generate entanglement but only for modes with wave vectors $|k| \leq \Lambda e^u$.

The expressions for these operators will be presented as necessary in the following presentation. However for this point it is sufficient to say that both are integrals over local densities which are combinations of the field operators, their adjoints and their derivatives of the specific quantum field theory in question.

It will be useful in the following sections to utilise the interaction picture for these unitary operators. This amounts to:

$$U(u_1, u_2) = e^{-iu_1 L} \cdot P \exp \left(-i \int_{u_2}^{u_1} \hat{K}(u) du \right) \cdot e^{iu_2 L}, \quad (4.31)$$

where we've defined:

$$\hat{K}(u) \equiv e^{iuL} \cdot K(u) \cdot e^{-iuL}. \quad (4.32)$$

4.1.1 Scalar Field Theory

The first example which we will consider is cMERA applied to a free relativistic massive scalar field theory in $(d+1)$ -dimensions. The Hamiltonian for this theory is given by:

$$H = \frac{1}{2} \int d^d k [\pi(k)\pi(-k) + \varepsilon_k^2 \phi(k)\phi(-k)], \quad (4.33)$$

where the fields satisfy the usual commutation relations and the dispersion relation is given by:

$$\varepsilon_k = \sqrt{|k|^2 + m^2}. \quad (4.34)$$

⁵In some of the literature this is written as a time ordering, however since the time in question is not strictly a time but rather a scale parameter or computational "time" we will refer to it as path ordering.

The scale transformation and disentangler in momentum space are given by [8] :

$$L = \frac{i}{2} \int d^d k [\phi(-k)|k|\pi(k) - |k|\pi(-k)\phi(k)], \quad (4.35)$$

$$K(u) = \frac{1}{2} \int d^d k [g(k, u) (\phi(k)\pi(-k) + \pi(k)\phi(-k))]. \quad (4.36)$$

The function $g(k, u)$ imposes the cut-off for the disentangling operator such that it only acts at the correct length scale. Moreover it is a dimensionless function which is even (odd) in k for bosons (fermions). In the literature it is parametrised as some even (odd) polynomial in k/Λ with s -dependent coefficients all multiplied by a constant cut-off function. This would call for the following functional form:

$$g(k, u) = \gamma(k/\Lambda, u) \cdot \Gamma(|k|/\Lambda). \quad (4.37)$$

However, in the examples which we will (re)derive it is sufficient to terminate the polynomial function at lowest order of k/Λ thereby allowing us to use for bosons:

$$g(k, u) = \chi(u) \cdot \Gamma(|k|/\Lambda), \quad (4.38)$$

where $\chi(u)$ is real-valued and Γ enacts the cut-off. For fermions $g(k, u)$ will have a factor of k/Λ multiplying $\chi(u)$ from the lowest order term in k . For the analytic results that follow a sharp Heavyside function is taken for clarity. By using a cut-off function, the disentangler will be only local up to factors of $\mathcal{O}(\Lambda^{-1})$, this can be avoided by taking the disentangler strictly to be polynomial in k and to use smoothed operators⁶. This effectively defines the cMERA ansatz to determine the ground state of the Hamiltonian.⁷ Now taking the interaction picture we can determine that:

$$\begin{aligned} \hat{K}(u) &= \frac{1}{2} \int d^d k e^{du} [g(k, u)\phi(ke^u)\pi(-ke^u) + g(k, u)\pi(ke^u)\phi(-ke^u)], \\ &= \frac{1}{2} \int d^d k [g(ke^{-u}, u) (\phi(k)\pi(-k) + \pi(k)\phi(-k))], \end{aligned} \quad (4.39)$$

where we have used the action of the scale transformation on the fields:

$$e^{-iuL} \cdot \phi(k) \cdot e^{iuL} = e^{-\frac{d}{2}u}\phi(ke^{-u}); \quad e^{-iuL} \cdot \pi(k) \cdot e^{iuL} = e^{-\frac{d}{2}u}\pi(ke^{-u}). \quad (4.40)$$

Now we can apply the full unitary operator to the fields, yielding:

$$\begin{aligned} U(0, u)^{-1} \cdot \phi(k) \cdot U(0, u) &= e^{-f(k, u)} e^{-\frac{d}{2}u}\phi(ke^{-u}), \\ U(0, u)^{-1} \cdot \pi(k) \cdot U(0, u) &= e^{f(k, u)} e^{-\frac{d}{2}u}\pi(ke^{-u}). \end{aligned} \quad (4.41)$$

The function appearing, $f(k, u)$, satisfies the equation:

$$\frac{\partial f(k, u)}{\partial u} = g(ke^{-u}, u), \quad (4.42)$$

which is directly solved by the integral:

$$f(k, u) = \int_0^u g(ke^{-s}, s) ds. \quad (4.43)$$

⁶For a further discussion on this point please refer to the appendix of version 1 of [47]

⁷This will in fact produce the exact ground state.

To determine the functional form of $f(k, u)$ we apply the variational principle to minimize the energy functional:

$$\begin{aligned}
E &= \langle \Psi | H | \Psi \rangle, \\
&= \langle \Omega | U^\dagger(0, u_{IR}) H U(0, u_{IR}) | \Omega \rangle, \\
&= \langle \Omega | H(u_{IR}) | \Omega \rangle, \\
&= \langle \Omega | \frac{1}{2} \int d^d k e^{2f(k, u_{IR})} e^{-u_{IR}d} \pi(k e^{-u_{IR}}) \pi(-k e^{-u_{IR}}) \\
&\quad + \varepsilon_k^2 e^{-2f(k, u_{IR})} e^{-u_{IR}d} \phi(k e^{-u_{IR}}) \phi(-k e^{-u_{IR}}) | \Omega \rangle, \\
&= \int d^d k \frac{1}{4} \left[e^{2f(k, u_{IR})} M + \frac{\varepsilon_k^2}{M} e^{-2f(k, u_{IR})} \right] \delta^d(0), \\
e &= E / \int d^d x = \int d^d k \frac{1}{4} \left[e^{2f(k, u_{IR})} M + \frac{\varepsilon_k^2}{M} e^{-2f(k, u_{IR})} \right]. \tag{4.44}
\end{aligned}$$

In the first lines we have used the operator and state scaling under cMERA (4.27),(4.29). Later we have used the previous definition (4.24) and properties (4.26) of the IR state. In the final line we exchange the d -dimensional delta function for a real space volume. Now we minimize the energy density functional with respect to $\chi(u)$ for any value of u :

$$\frac{\delta e}{\delta \chi(u)} = \int d^d k \left[e^{2f(k, u_{IR})} M - \frac{\varepsilon_k^2}{M} e^{-2f(k, u_{IR})} \right] \Gamma(|k| e^{-u} / \Lambda) = 0, \tag{4.45}$$

where the we have used that:

$$\frac{\delta f(k)}{\delta \chi(u)} = \Gamma(|k| e^{-u} / \Lambda), \tag{4.46}$$

by using the integral form of $f(k, u)$ and so on. Since this holds for any value of u we find that:

$$\begin{aligned}
\left[e^{2f(k, u_{IR})} M - \frac{\varepsilon_k^2}{M} e^{-2f(k, u_{IR})} \right] &= 0, \\
\Rightarrow f(k, u_{IR}) &= \frac{1}{2} \log \frac{\varepsilon_k}{M}, \tag{4.47}
\end{aligned}$$

for momenta below the cut-off. Next recall the integral solution of $f(k, u)$ at the infrared limit:

$$\begin{aligned}
f(k, u_{IR}) &= \int_0^{u_{IR}} g(k e^{-s}, s) ds, \\
&= \int_0^{u_{IR}} \chi(s) \Gamma(|k| e^{-s} / \Lambda) ds, \\
&= \int_0^{u_{IR}} \chi(s) \Theta(1 - |k| e^{-s} / \Lambda) ds, \\
\Rightarrow f(k, u_{IR}) &= \int_0^{-\log(\Lambda/|k|)} \chi(s) ds. \tag{4.48}
\end{aligned}$$

Now we combine these two expressions for $f(k)$ and take the derivative with respect to k to find that:

$$\chi(u) = \frac{1}{2} \left(\frac{|k| \partial_{|k|} \varepsilon_k}{\varepsilon_k} \right) \Big|_{|k| = \Lambda e^u}. \tag{4.49}$$

Notice that the actual form of the dispersion relation was not used in the steps to find this expression and in fact the above expression holds for a general dispersion relation which allows us to insert whatever relation is of interest. This function $\chi(u)$ will characterise the ground

state of the field theory. For the free relativistic field theory we started with the function evaluates to:

$$\begin{aligned}\chi(u) &= \frac{1}{2} \left(\frac{|k|k}{\varepsilon_k^2} \right)_{|k|=\Lambda e^u}, \\ &= \frac{1}{2} \left(\frac{\Lambda^2 e^{2u}}{\Lambda^2 e^{2u} + m^2} \right), \\ &= \frac{1}{2} \left(\frac{e^{2u}}{e^{2u} + (m^2/\Lambda^2)} \right).\end{aligned}\tag{4.50}$$

Using this final expression we can readily integrate the expression to recover $f(k, u)$ both above and below the momentum cut-off:

$$f(k, u) = \begin{cases} \frac{1}{4} \log \frac{\Lambda^2 e^{2u} + m^2}{\Lambda^2 + m^2}, & (|k| < \Lambda e^u) \\ \frac{1}{4} \log \frac{k^2 + m^2}{\Lambda^2 + m^2}. & (|k| > \Lambda e^u) \end{cases}\tag{4.51}$$

Since $\chi(u)$ characterises the ground state it is worth noting some limits of this function. For example if we want to examine a scalar conformal field theory we can take the massless limit thereby finding a constant value for the function:

$$\chi_{m=0} = \frac{1}{2}.\tag{4.52}$$

This is interesting as it indicates that the full unitary transformation of $K + L$ is equivalent to a scale transformation or dilatation in the massless limit. For the massive case we find a similar result in the UV region⁸ in which $\chi(u) \approx \frac{1}{2}$. However in the IR region we find that the function approaches zero, indicating a trivial action of the unitary operator and thus the absence of a mass gap.

Having found $f(k, u_{IR})$ by variational methods (4.47) it is worth checking what this yields for the expression (4.44) we had for the energy density. Inserting into the expression for the energy we find:

$$\begin{aligned}e &= \int d^d k \frac{1}{4} \left[e^{2f(k, u_{IR})} M + \frac{\varepsilon_k^2}{M} e^{-2f(k, u_{IR})} \right], \\ &= \int d^d k \frac{1}{4} \left[\frac{\varepsilon_k}{M} M + \frac{\varepsilon_k^2}{M \varepsilon_k} M \right], \\ &= \int d^d k \frac{1}{4} [\varepsilon_k + \varepsilon_k], \\ &= \int d^d k \frac{1}{2} \varepsilon_k.\end{aligned}\tag{4.53}$$

This passes our sanity check since we have effectively recovered the energy density of an infinite number of harmonic oscillators with dispersion relation ε_k in natural units.

4.1.2 An Emergent Metric

While one may make qualitative comparisons [6] between AdS space and the structure of a MERA network it has been found that by applying continuous MERA techniques to free field theories one may in effect produce an emergent metric for such an AdS space. The full

⁸We mean here that $e^u \gg m/\Lambda$.

justification of this claim is found in the literature [8] wherein the metric element g_{uu} can be expressed as:

$$g_{uu}(u) = \langle \Phi(u) | \hat{K}(u)^2 | \Phi(u) \rangle - \langle \Phi(u) | \hat{K}(u) | \Phi(u) \rangle^2, \quad (4.54)$$

where $|\Phi(u)\rangle \equiv e^{iuL} |\Psi(u)\rangle$. This expression is found by defining the Hilbert-Schmidt distance between two cMERA states at infinitesimally different scales the result of this procedure may then be expressed as the variance above.

For this thesis we take the result that if we consider the ground state of the free field theory then the metric element corresponding to the holographic direction, g_{uu} , is related to the function $\chi(u)$, which we are able to determine, as follows:

$$g_{uu}(u) = \chi^2(u). \quad (4.55)$$

Thus by determining the function $\chi(u)$ via cMERA methods one determines the dual AdS metric. The x component of the metric will be determined by the coarse graining procedure so that we have:

$$ds^2 = g_{uu} du^2 + \frac{e^{2u}}{\epsilon^2} d\vec{x}^2 + g_{tt} dt^2. \quad (4.56)$$

Since we maintain the same coarse graining procedure throughout the cMERA discussions the metric component remains fixed as above. As for the temporal component this will not be relevant for the entanglement entropy calculations. However, if the entanglement entropy is generalised such that the subsystem A is defined on a Lorentz boosted time slice then in principle the g_{tt} may be read off [8]. This is only mentioned for completeness as we will not address this aspect further in this thesis.

Scalar Field

Then, continuing from (4.55) we can determine the metric and by extension the entanglement entropy for a scalar field theory. In the previous section we determined $\chi(u)$ (4.50), thereby giving us the metric element for the dual metric:

$$g_{uu}(u) = \chi^2(u) = \frac{e^{4u}}{4(e^{2u} + m^2/\Lambda^2)^2}. \quad (4.57)$$

At the moment this is not quite what we expect for the metric of AdS space. To make the connect more clear we introduce the coordinate change defined by:

$$e^{2u} = \frac{1}{\Lambda^2 z^2} - \frac{m^2}{\Lambda^2}, \quad (4.58)$$

where $0 < z < 1/m$, which yields:

$$\begin{aligned} g_{uu} du^2 &= \frac{e^{4u}}{4 \left(\frac{1}{\Lambda^2 z^2} - \frac{m^2}{\Lambda^2} + \frac{m^2}{\Lambda^2} \right)^2} \cdot \frac{4e^{-4u} dz^2}{\Lambda^2 z^4 4z^2}, \\ &= \frac{\Lambda^4 z^4 e^{4u}}{4} \cdot \frac{4e^{-4u} dz^2}{\Lambda^2 z^4 4z^2}, \\ &= \frac{dz^2}{4z^2}. \end{aligned} \quad (4.59)$$

Recall that $\Lambda = 1/\epsilon$ to arrive at the metric:

$$ds^2 = \frac{dz^2}{4z^2} + \left(\frac{1}{z^2} - \frac{m^2}{\Lambda^2} \right) dx^2 + g_{tt} dt^2. \quad (4.60)$$

The metric vanishes at $z = 1/m$ which is consistent with the mass gap of the scalar field theory. Moreover, taking the massless case we can see that a pure AdS metric is recovered.⁹

⁹Up to a small coordinate rescaling.

Chapter 5

cMERA and Lifshitz Theories

5.1 Lifshitz Scaling

In this chapter we will extend the results discussed in the previous chapter to theories with Lifshitz scaling. Up until now we have only studied situations in which local interactions are the only interactions of consequence. However we are also interested in long range interactions. One way to achieve this is to introduce Lifshitz scaling to the system at hand. This effectively amounts to a skewing of the massless scale invariance which we have seen previously. Rather than space-time transforming under rescaling in an equal way the scaling becomes skewed such that time and space are scaled in a different manner. The Lifshitz scale invariance reads as:

$$t \rightarrow \lambda^\nu t, \quad x \rightarrow \lambda x. \quad (5.1)$$

The variable ν^1 is known as the dynamical critical exponent.

For a scalar field theory this scaling amounts to the following change to the general dispersion relation seen previously (4.34):

$$\varepsilon_k = \sqrt{k^{2\nu} + m^2} \quad (5.2)$$

The changes seen in fermionic theories will be introduced in the relevant section. For now we will examine the entanglement entropy for a Lifshitz scalar field using cMERA methods.

5.2 Scalar Field

Much of this section is an expanded presentation to that found in recent work [55], further results may be found in [56].

From [8] we have that the bulk metric from cMERAs of non-CFTs are given by:

$$ds^2 = g_{uu} du^2 + \frac{e^{2u}}{\varepsilon^2} d\vec{x}^2 + g_{tt} dt^2. \quad (5.3)$$

Note that we used a rather than ε for the cut-off previously. For pure AdS we have $g_{uu} = 1$ and Poincaré coordinates $z = \varepsilon \cdot e^{-u}$, $g_{tt} = -\varepsilon \cdot e^{-u}$. This yields:

$$ds^2 = \frac{1}{z^2} \left(-dt^2 + dz^2 + d\vec{x}^2 \right). \quad (5.4)$$

Here $z \rightarrow 0$ corresponds to the boundary of AdS space. The continuous limit is found by $\varepsilon \rightarrow 0$.

¹In a great deal of literature this is denoted by z . Here we will use ν as z is used in several other situations already.

In [8] it is demonstrated that for free scalar fields with dispersion relation ε_k we can find the metric element g_{uu} via the relation:

$$g_{uu}(u) = \chi(u)^2; \chi = \frac{1}{2} \left(\frac{|k| \partial_{|k|} \varepsilon_k}{\varepsilon_k} \right)_{|k|=\Lambda e^u}. \quad (5.5)$$

This metric is supposed to be dual to the ground state of the field theory by conjecture. Furthermore the cut-off of the field theory is identified as: $\Lambda = \frac{1}{\varepsilon}$.

For massive Lifshitz scalar fields we have the following dispersion relation where ν is the dynamical exponent:

$$\varepsilon^2(k) = k^{2\nu} + m^2 \rightarrow \varepsilon_k = \sqrt{k^{2\nu} + m^2}. \quad (5.6)$$

It should be noted that the dynamical exponent is often denoted by z [55] and there is usually a factor of $\alpha^2 = 1/c^2$ for $\nu = 1$ in the field theory that has been set to one here for convenience. In general $[\alpha] = m^\nu/s$.

Following the literature for simplicity we look at the (1+1) dimensional case but additional x dimensions should be straightforward to realise conceptually. So evaluating $\chi(u)$ we find:

$$\chi(u) = \frac{\nu}{2} \left(\frac{e^{2u\nu}}{e^{2u\nu} + M^2} \right), \quad (5.7)$$

where $M = \frac{m}{\Lambda^\nu} = m\varepsilon^\nu$. This is denoted as J in other sources [55].

We concern ourselves with the spatial part of the metric as we are interested in time slices of AdS i.e. cMERA. In any case the time component is not necessary for Entanglement Entropy for time-independent states naturally. Thus:

$$ds^2 = \frac{\nu^2}{4} \frac{e^{4u\nu}}{(e^{2u\nu} + M^2)^2} du^2 + \frac{e^{2u}}{\varepsilon^2} dx^2. \quad (5.8)$$

Now we perform the coordinate transformation:

$$e^{2u\nu} + M^2 = \frac{\varepsilon^2}{z^2},$$

notice that for zero mass and ν set to 1 we recover the same transformation as for pure AdS seen already(4.58). Performing this transformation however gives the result:

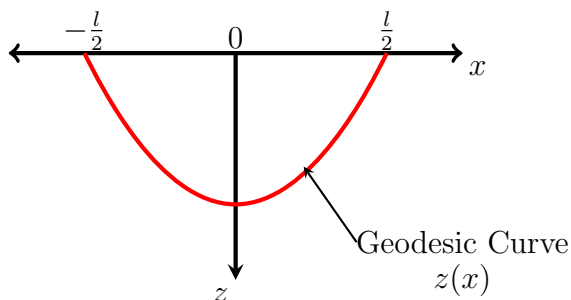
$$ds^2 = \frac{1}{4} \frac{dz^2}{z^2} + \left(\frac{\varepsilon^2}{z^2} - M^2 \right)^\frac{1}{\nu} \frac{dx^2}{\varepsilon^2}. \quad (5.9)$$

At this point it is useful to find the range of values which this z -coordinate may take. From cMERA we know that $u \in \{0, -1, \dots -\infty\}$ and in particular: $u_{UV} = 0$ and $u_{IR} = -\infty$.

From the coordinate transformation we can see that these values translate to:

$$z_{UV} = \frac{\varepsilon}{\sqrt{1 + M^2}}, \quad z_{IR} = \frac{\varepsilon}{M}. \quad (5.10)$$

Notice that the geometry now has a cut-off due to the mass. If the mass is sent to zero then $z_{IR} \rightarrow \infty$.



Now Ryu-Takayanagi techniques are used in the minimization of geodesics to compute the entanglement entropy. The geometric picture to have in mind is shown above.

The relevant metric from which we compute the geodesic length will then be:

$$ds^2 = \left(\frac{1}{4z^2} \frac{dz^2}{dx^2} + \left(\frac{\varepsilon^2}{z^2} - M^2 \right)^{\frac{1}{\nu}} \frac{1}{\varepsilon^2} \right) dx^2. \quad (5.11)$$

By convention this is a dimensionless quantity as the EE which we computed by minimizing the following pseudo-action:

$$S = \int_{-\frac{l}{2}}^{\frac{l}{2}} dx \sqrt{\frac{1}{4} \frac{z'^2}{z^2} + \frac{1}{\varepsilon^2} \left(\frac{\varepsilon^2}{z^2} - M^2 \right)^{\frac{1}{\nu}}}. \quad (5.12)$$

Interpreting x as a "time" we can say that the Lagrangian is

$$\mathcal{L} = \sqrt{\frac{1}{4} \frac{z'^2}{z^2} + \frac{1}{\varepsilon^2} \left(\frac{\varepsilon^2}{z^2} - M^2 \right)^{\frac{1}{\nu}}}. \quad (5.13)$$

Furthermore a pseudo-Hamiltonian may be constructed by the usual method:

$$\mathcal{H} = p_z z' - \mathcal{L}, \quad p_z = \frac{\partial \mathcal{L}}{\partial z'} = \frac{1}{4\mathcal{L}} \frac{z'}{z^2}. \quad (5.14)$$

This then yields the following expression for the Hamiltonian after some manipulations:

$$\begin{aligned} \mathcal{H}(p_z, z) &= \frac{1}{4\mathcal{L}} \frac{z'}{z^2} \cdot z' - \mathcal{L}, \\ &= \frac{1}{\mathcal{L}} \left(\frac{1}{4} \frac{z'^2}{z^2} - \mathcal{L}^2 \right), \\ &= \frac{1}{\mathcal{L}} \left(\frac{1}{4} \frac{z'^2}{z^2} - \frac{1}{4} \frac{z'^2}{z^2} - \frac{1}{\varepsilon^2} \left(\frac{\varepsilon^2}{z^2} - M^2 \right)^{\frac{1}{\nu}} \right), \\ &= \frac{1}{\mathcal{L}} \left(-\frac{1}{\varepsilon^2} \left(\frac{\varepsilon^2}{z^2} - M^2 \right)^{\frac{1}{\nu}} \right). \end{aligned} \quad (5.15)$$

Now notice that:

$$\begin{aligned} \varepsilon(1 - 4p_z^2 z^2) &= \varepsilon \left(1 - \frac{1}{4} \frac{z'^2}{\mathcal{L}^2 z^4} z^2 \right), \\ &= \frac{\varepsilon}{\mathcal{L}^2} \left(\mathcal{L}^2 - \frac{z'^2}{4z^2} \right), \\ &= \frac{\varepsilon}{\mathcal{L}^2} \left(\frac{1}{\varepsilon^2} \left(\frac{\varepsilon^2}{z^2} - M^2 \right)^{\frac{1}{\nu}} \right), \\ \mathcal{L}^2 &= \frac{1}{\varepsilon(1 - 4p_z^2 z^2)} \left(\frac{\varepsilon^2}{z^2} - M^2 \right)^{\frac{1}{\nu}}, \\ \mathcal{L} &= \frac{1}{\varepsilon \sqrt{(1 - 4p_z^2 z^2)}} \left(\frac{\varepsilon^2}{z^2} - M^2 \right)^{\frac{1}{2\nu}}. \end{aligned} \quad (5.16)$$

Inserting this form of the Lagrangian into the last expression for the Hamiltonian yields the result:

$$\mathcal{H} = -\frac{1}{\varepsilon} \sqrt{(1 - 4p_z^2 z^2) \left(\frac{\varepsilon^2}{z^2} - M^2 \right)^{\frac{1}{\nu}}} =: E. \quad (5.17)$$

This is a constant of motion as \mathcal{H} does not depend on x explicitly. We define this as the quantity E , since it manifestly has dimension of inverse length and hence that of energy.

This step is unverified but apparently a rewriting of $\mathcal{H} = E$ gives the differential equation for z :

$$\frac{dz}{dx} = \sqrt{\frac{4z^2}{\varepsilon^2} \frac{1}{\varepsilon^2 E^2} \left(\frac{\varepsilon^2}{z^2} - M^2 \right)^{\frac{2}{\nu}} - \frac{4z^2}{\varepsilon^2} \left(\frac{\varepsilon^2}{z^2} - M^2 \right)^{\frac{1}{\nu}}}. \quad (5.18)$$

We now take dimensionless variables instead for clarity in the proceeding manipulations:

$$\tilde{z} \equiv \frac{z}{\varepsilon}, \tilde{x} \equiv \frac{x}{\varepsilon}, \tilde{E} \equiv \varepsilon \cdot E. \quad (5.19)$$

Replace these variable in the pseudo-action and the differential equation being sure to rescale the limits appropriately. Dropping the tildes after yields:

$$\tilde{S} = \int_{-\frac{1}{2\varepsilon}}^{\frac{1}{2\varepsilon}} dx \sqrt{\frac{z'^2}{4z^2} + \left(\frac{1}{z^2} - M^2 \right)^{\frac{1}{\nu}}}, \quad (5.20)$$

and

$$\frac{dz}{dx} = \sqrt{\frac{4z^2}{E^2} \left(\frac{1}{z^2} - M^2 \right)^{\frac{2}{\nu}} - 4z^2 \left(\frac{1}{z^2} - M^2 \right)^{\frac{1}{\nu}}}. \quad (5.21)$$

The differential equation may then be taken into the following form:

$$\frac{dz}{dx} = \frac{2z}{E} \left(\frac{1}{z^2} - M^2 \right)^{\frac{1}{\nu}} \sqrt{1 - q}, \quad (5.22)$$

where we've defined $q \equiv E^2 \left(\frac{1}{z^2} - M^2 \right)^{\frac{-1}{\nu}}$.

Since $1 - q \geq 0$ the turning point is given by: $z_* = \frac{1}{\sqrt{E^{2\nu} + M^2}}$ and $0 = q_{UV} \leq q \leq q_{IR} = \infty$. Moreover we can express the defining equation of q as $z^2 = \frac{q^\nu}{E^{2\nu} + M^2 q^\nu}$. Using this relation we can change variables $dz \rightarrow dq$ to find:

$$\frac{4E}{\nu} \int dx + \text{const.} = \int \frac{dq}{\sqrt{1 - q} \left(1 + q^\nu \left(\frac{M}{E^\nu} \right)^2 \right)}. \quad (5.23)$$

The right-hand side cannot be solved in closed form for non-zero mass and $\nu \neq 1$ so we look at the massless case to find that:

$$-2\sqrt{1 - q} = \frac{4Ex}{\nu} + \text{constant}. \quad (5.24)$$

From the geometric set up we have a symmetry about the holographic direction i.e. under $x \rightarrow -x$. This fixes the constant to be zero. (This is the translation invariance of the problem manifest.) Thus,

$$4(1 - q) = \left(\frac{4Ex}{\nu} \right)^2.$$

Furthermore this gives us a suggestive equation, using $q = z^{\frac{2}{\nu}} E^2$,

$$\left(z^{\frac{1}{\nu}} \right)^2 + \left(\frac{2x}{\nu} \right)^2 = \frac{1}{E^2}, \quad (5.25)$$

and recalling a simple identity we can solve this using:

$$\begin{aligned} z(s) &= \frac{1}{E^\nu} \sin^\nu(s), \\ x(s) &= -\frac{\nu}{2E} \cos(s). \end{aligned} \quad (5.26)$$

Using the UV cut-off established we have $x(0) = -\frac{l}{2\varepsilon} = -\frac{\nu}{2E}$. Hence $E = \frac{\nu\varepsilon}{l}$ and $z_* = \frac{l}{\varepsilon}$ for $\nu = 1$ or $z_* = l$ if we rescale back to the original variables. The angle of integration s runs over $0 \rightarrow \pi$ but we can integrate twice over $0 \rightarrow \frac{\pi}{2}$ by symmetry if we prefer, which we do.

The massless pseudo-action is:

$$\tilde{S}_{m=0} = \int_{\frac{l}{2\varepsilon}}^{\frac{l}{2\varepsilon}} dx \sqrt{\frac{z'^2}{4z^2} + \frac{1}{z^{\frac{2}{\nu}}}}. \quad (5.27)$$

Now we change variables to integrate over the angle instead of x .

$$\begin{aligned} \frac{dx}{ds} &= \frac{\nu}{2E} \sin(s), \\ z' &= \frac{dz}{ds} \cdot \frac{ds}{dx} = \left(\frac{\nu}{E^\nu} \sin^{\nu-1} \cos(s) \right) \left(\frac{2E}{\nu} \frac{1}{\sin(s)} \right), \\ &= \frac{2}{E^{\nu-1}} \cos(s) \sin^{\nu-2}(s), \\ \frac{z'^2}{4z^2} + \frac{1}{z^{\frac{2}{\nu}}} &= E^2 \frac{\cos^2(s)}{\sin^4(s)} + \frac{E^2}{\sin^2(s)}, \\ \sqrt{\frac{z'^2}{4z^2} + \frac{1}{z^{\frac{2}{\nu}}}} &= \frac{E}{\sin^2(s)}, \\ dx &= \frac{\nu}{2E} \sin(s) ds. \end{aligned} \quad (5.28)$$

This leaves us with the result for the Entanglement Action:

$$\begin{aligned} \tilde{S}_{m=0} &= 2 \cdot \int_0^{\frac{\pi}{2}} ds \frac{\nu}{2E} \sin(s) \frac{E}{\sin^2(s)}, \\ &= \nu \int_\alpha^{\frac{\pi}{2}} \frac{ds}{\sin(s)}, (\alpha \rightarrow 0). \end{aligned} \quad (5.29)$$

We've inserted α here which will be the dimensionless cut-off for the integral since this integral is divergent at zero. However with the cut-off we can use the indefinite answer:

$$\tilde{S}_{m=0} = \nu \left[-\log\left(\cos\left(\frac{s}{2}\right)\right) + \log\left(\sin\left(\frac{s}{2}\right)\right) \right]_\alpha^{\frac{\pi}{2}}. \quad (5.30)$$

The upper limit is manifestly zero so we only need to look at the lower limit. Note also that $\log\left(\cos\left(\frac{\alpha}{2}\right)\right) \rightarrow 0$ as $\alpha \rightarrow 0$. Therefore,

$$\tilde{S}_{m=0} = -\nu \log\left(\sin\left(\frac{\alpha}{2}\right)\right) \approx -\nu \log\left(\frac{\alpha}{2}\right). \quad (5.31)$$

Now we need to determine the value of α . It should be dimensionless and proportional to the UV cut-off ε . Recall, $z_{UV} = \varepsilon$. Equivalently, $\tilde{z}_{UV} = 1$. We have an expression for this, $\tilde{z} = \frac{1}{E^\nu} \sin^\nu(s)$. So then, $1 = \frac{1}{E^\nu} \sin^\nu(\alpha) \approx \frac{\alpha^\nu}{E^\nu}$. This gives:

$$\alpha = E = \frac{\nu\varepsilon}{l}. \quad (5.32)$$

The entanglement entropy is then:

$$S_{EE} = -\nu \log\left(\frac{\nu\varepsilon}{2l}\right) = \nu \log\left(\frac{2l}{\nu\varepsilon}\right). \quad (5.33)$$

Usually, we redefine the cut-off so that any constant factors in the argument of the log are absorbed.

The final step here is to fix the normalisation of the action to obtain the correct value of the entanglement entropy. Comparing to the $\nu = 1$ case we find that:

$$S_{EE} = \frac{\nu}{3} \log\left(\frac{l}{\nu\varepsilon}\right), \quad (5.34)$$

having also redefined ε to absorb the factor of 2. One should notice that this is not the whole story. The expression above will only be valid for “small” values of ν such that $\nu\varepsilon$ is not of the same order as l . The result in full generality for a massless free scalar field has been found recently [56] and is given by:

$$S_{EE} = \frac{\nu}{3} \log\left(\frac{l}{\nu\varepsilon} + \sqrt{\left(\frac{l}{\nu\varepsilon}\right)^2 + 1}\right). \quad (5.35)$$

Expanding around large ν or equivalently, small $l/\nu\varepsilon$ one finds small deviations from a volume law:

$$S_{EE} = \frac{l}{\nu\varepsilon} \left[1 - \frac{1}{6} \left(\frac{l}{\nu\varepsilon}\right)^2 + \mathcal{O}\left(\frac{l}{\nu\varepsilon}\right)^4\right]. \quad (5.36)$$

For small ν one finds small deviations from an area law:

$$S_{EE} = \frac{\nu}{3} \left[\log\left(\frac{l}{\nu\varepsilon}\right) + \log(2) + \mathcal{O}\left(\frac{\nu\varepsilon}{l}\right)^2 + \dots\right]. \quad (5.37)$$

Now we tackle the massive case. Consider the relativistic case for ease of calculation i.e. $\nu = 1$. Our starting point will be the q integral of eqn (14).

$$4Ex + c = \int \frac{dq}{\sqrt{1-q} \left(1 + q \left(\frac{M}{E}\right)^2\right)}. \quad (5.38)$$

To solve this we begin by making the substitution: $y = \sqrt{1-q}$, to give

$$\begin{aligned} 4Ex + c &= -2 \int \frac{dy}{1 + (1-y^2) \left(\frac{M}{E}\right)^2}, \\ &= -2 \int \frac{dy}{a^2 - b^2 y^2}, \\ &= -2 \int \frac{1}{a^2} \frac{dy}{1 - \frac{b^2}{a^2} y^2}, \\ &= -2 \int \frac{1}{ab} \frac{d\omega}{1 - \omega^2}, \\ &= -\frac{1}{ab} \int d\omega \left[\frac{1}{1-\omega} + \frac{1}{1+\omega} \right], \\ &= -\frac{1}{ab} \log \left[\frac{a+by}{a-by} \right], \end{aligned}$$

where we've made the following substitutions in various steps:

$$a = \sqrt{1 + \frac{M^2}{E^2}}, b = \frac{M}{E}, \omega = \frac{b}{a}y.$$

Now we would like to massage this relation into a similarly suggestive equation as we found in the massless case so that we may parametrize $z = z(s)$ and $x = x(s)$.

$$\begin{aligned} 4Ex + c &= -\frac{1}{ab} \log \left[\frac{a + by}{a - by} \right], \\ -4abEx - abc &= \log \left[\frac{a + by}{a - by} \right], \\ e^{-abc} e^{-4abEx} &= \left[\frac{a + by}{a - by} \right]. \end{aligned}$$

By translation invariance i.e. $x \rightarrow -x$ we have as before that $c = 0$ and hence $e^{-abc} = 1$. Then solving for y we find that:

$$y = \frac{a}{b} \left(\frac{e^{-4abEx} - 1}{e^{-4abEx} + 1} \right). \quad (5.39)$$

Now for the moment let us label the bracketed fraction by e and recall the definition of q in terms of y and z . Then we perform some algebra:

$$\begin{aligned} 1 - y^2 = q &= E^2 \left(\frac{1}{z^2} - M^2 \right)^{-1}, \\ 1 - \frac{a^2}{b^2} e^2 &= E^2 \left(\frac{1}{z^2} - M^2 \right)^{-1}, \\ E^2 &= \frac{1}{z^2} \frac{b^2 - a^2 e^2}{b^2} - M^2 \frac{(b^2 - a^2 e^2)}{b^2}, \\ \frac{1}{z^2} &= \frac{E^2 b^2}{b^2 - a^2 e^2} + M^2, \\ z^2 &= \frac{b^2 - a^2 e^2}{E^2 b^2 + M^2 b^2 - M^2 a^2 e^2}, \\ z^2 &= \frac{M^2 (1 - e^2) + e^2 E^2}{M^2 E^2 (1 - e^2) + M^4 (1 - e^2)}, \\ z^2 &= \frac{1}{E^2 + M^2} - \frac{e^2}{(1 - e^2)} \frac{E^2}{M^2} E^2 + M^2, \\ z^2 &= \frac{1}{a^2 E^2} - \frac{1}{a^2 b^2 E^2} \sinh^2(2abEx). \end{aligned}$$

This final line is the suggestive form we were aiming to find. The combination of $\frac{e^2}{1 - e^2}$ is found to be equal to $\sinh^2(2abEx)$ by liberal use of trigonometric identities. Other than this the remainder of the manipulation is achieved by substituting different combinations of the energy and mass. As a consistency check one can set $b = 0$ and $a = 1$ to recover the massless case, one can easily verify that $\lim_{a \rightarrow 1} \lim_{b \rightarrow 0} \frac{\sinh^2(2abEx)}{a^2 b^2} = 4E^2 x^2$. Likewise for the following parametrizations.

From this form we propose the parametrization:

$$z(s) = \frac{1}{aE} \sin(s), x(s) = -\frac{1}{2abE} \operatorname{arcsinh}[b \cos(s)]. \quad (5.40)$$

Proceeding in the same manner as previously we obtain the Entanglement Action:

$$\begin{aligned}
S_{EE} &= \frac{1}{3} \int_{-\frac{l}{2\varepsilon}}^{\frac{l}{2\varepsilon}} dx \sqrt{\frac{z'^2}{4z^2} + \left(\frac{1}{z^2} - M^2\right)}, \\
&= 2 \times \frac{a}{4b} \times \frac{1}{3} \int_0^{\frac{\pi}{2}} ds \frac{1}{\sin(s)} \sqrt{\frac{\cos^2(s)(1 + b^2 \cos^2(s)) + 4 \sin^2(s)(1 - M^2 \sin^2(s))}{1 + b^2 \cos^2(s)}}.
\end{aligned} \tag{5.41}$$

The result of this integral is not immediately obvious so first we can look at the UV-behaviour of the parameters to determine the values of $s = \alpha$ and E . Being sure to keep track of rescaling that has been done we recall that $z_{UV} = \frac{1}{\sqrt{1+M^2}}$ and using the parametrization we have for small s :

$$\begin{aligned}
\frac{1}{\sqrt{1+M^2}} &= \frac{1}{aE} \alpha, \\
\alpha &= \frac{aE}{\sqrt{1+M^2}} = \sqrt{\frac{E^2 + M^2}{1+M^2}}.
\end{aligned}$$

Similarly for the space direction:

$$\begin{aligned}
x_{UV} &= \frac{l_A}{2\varepsilon} = \frac{1}{2abE} \operatorname{arcsinh}(b), \\
\operatorname{arcsinh}\left(\frac{M}{E}\right) &= \frac{l_A M}{E\varepsilon} \sqrt{E^2 + M^2}, \\
\frac{M}{E} &= \sinh\left[N_A M \sqrt{1 + \frac{M^2}{E^2}}\right],
\end{aligned}$$

where we used that: $l_A = N_A \varepsilon$, $M = m\varepsilon$ so $N_A M = \frac{M}{\varepsilon} l_A$.

Solving then for E is not possible without some approximations. However there are two physical regimes depending on whether the correlation length is larger or smaller than the subsystem size l_A . These were initially proposed by Casini-Huerta [57] and Cardy-Calabrese [58] respectively.

First the Casini-Huerta regime. Here $\xi \gg l_A \gg \varepsilon$. Moreover, $N_A M = l_A m = l_A/\xi \ll 1$. Then $M \ll 1$ as we have $N_A \gg 1$. Given this information we know that we can expand $\sinh(x)$ around small x giving:

$$\frac{M}{E} \approx N_A M \sqrt{1 + \frac{M^2}{E^2}}, \tag{5.42}$$

taking $\frac{M}{E} = x$ we have:

$$\begin{aligned}
x^2 &= (N_A M)^2 (1 + x^2), \\
&= \frac{(N_A M)^2}{1 - (N_A M)^2} \ll 1, \\
\frac{M}{E} &\approx N_A M, \\
E &\approx \frac{1}{N_A}.
\end{aligned}$$

This also implies that $M \ll E$ so we have for α :

$$\alpha = \sqrt{\frac{E^2 + M^2}{1 + M^2}} \approx E. \tag{5.43}$$

Finally we see that $b \ll 1$ and $a \approx 1$.

Now for the Cardy-Calabrese regime. Here $l_A \gg \xi \gg \varepsilon$ so we have that $N_A M = l_A/\xi \gg 1$ and $M \ll 1$. Here since $N_A M$ is large we cannot make the expansion as before and indeed cannot take new information from the $x(s)$ expression so we look to the $z(s)$ expression instead. In the bulk near the IR we have $z(s) = N_A \sin(s)$ so that at the halfway point of the curve namely when deepest into the bulk geometry $z_* = N_A$. However we previously found that $z_{IR} = 1/M$ so since in this regime $N_A M \gg 1$, $M \ll 1$ this implies that $z_* \ll z_{IR}$. Meaning that the curve does not extend "too far" into the bulk geometry.

From the definition of q we have $q_* = \frac{1}{1-(N_A M)^2}$.

5.3 Dirac Field

Having addressed the case of a free scalar field we now turn our attention to the case of a free fermionic theory. First we proceed in a similar fashion as before 4.1 for the $\nu = 1$ case. The theory is described by the following Dirac Hamiltonian in $(1+1)$ -dimensions:

$$\begin{aligned} H &= \int dx \left[-i\bar{\psi}\gamma^x\partial_x\psi + m\bar{\psi}\psi \right], \\ &= \int dx \left[-i \begin{pmatrix} \psi_1^\dagger & \psi_2^\dagger \end{pmatrix} \begin{pmatrix} 0 & 1 \\ -1 & 0 \end{pmatrix} \begin{pmatrix} \partial_x\psi_1 \\ \partial_x\psi_2 \end{pmatrix} + m \begin{pmatrix} \psi_1^\dagger & \psi_2^\dagger \end{pmatrix} \begin{pmatrix} 1 & 0 \\ 0 & -1 \end{pmatrix} \begin{pmatrix} \psi_1 \\ \psi_2 \end{pmatrix} \right], \\ &= \int dx \left[-i(\psi_1^\dagger\partial_x\psi_2 - \psi_2^\dagger\partial_x\psi_1) + m(\psi_1^\dagger\psi_1 - \psi_2^\dagger\psi_2) \right], \end{aligned} \quad (5.44)$$

with $\bar{\psi} = \psi^\dagger\gamma^t$, $\gamma^t = \sigma^3$ and $\gamma^x = i\sigma^2$. Now our aim is to find the exact Bogoliubov angle which will eventually give us $\chi(s)$ necessary to obtain the metric element g_{uu} . First then we Fourier transform this Hamiltonian:

$$\begin{aligned} H &= \int dx \left[-i(\psi_1^\dagger\partial_x\psi_2 - \psi_2^\dagger\partial_x\psi_1) + m(\psi_1^\dagger\psi_1 - \psi_2^\dagger\psi_2) \right], \\ &= \int dx \int dk_1 \int dk_2 \left[-i \left(\psi_1^\dagger(k_1)e^{-ik_1x}\partial_x(\psi_2(k_2)e^{-ik_2x}) - \psi_2^\dagger(k_2)e^{ik_2x}\partial_x(\psi_1(k_1)e^{ik_1x}) \right) \right. \\ &\quad \left. + m \left(\psi_1^\dagger(k_1)\psi_1(k_1)e^{i(k_1-k_1)x} - \psi_2^\dagger(k_2)\psi_2(k_2)e^{i(k_2-k_2)x} \right) \right], \\ &= \int dx \int dk_1 \int dk_2 \left[-i \left(-ik_2\psi_1^\dagger(k_1)\psi_2(k_2)e^{-i(k_1+k_2)x} - (ik_1)\psi_2^\dagger(k_2)\psi_1(k_1)e^{i(k_1+k_2)x} \right) \right. \\ &\quad \left. + m \left(\psi_1^\dagger(k_1)\psi_1(k_1)e^{i(k_1-k_1)x} - \psi_2^\dagger(k_2)\psi_2(k_2)e^{i(k_2-k_2)x} \right) \right], \\ &= \int dk \left[k(\psi_1^\dagger(k)\psi_2(k) + \psi_2^\dagger(k)\psi_1(k)) + m(\psi_1^\dagger(k)\psi_1(k) - \psi_2^\dagger(k)\psi_2(k)) \right]. \end{aligned} \quad (5.45)$$

Our next step is to introduce new fields $\hat{\psi}_\alpha$ which are general Bogoliubov transformations of the original fields. These are in fact the fields under the action of the cMERA operator [47]. As such the momenta are rescaled also as we have the action of both $K(s)$ and L . These transformed fields are given by:

$$\hat{\psi}_1(k, s) = \cos(f(k, s))e^{-\frac{s}{2}}\psi_1(e^{-s}k) - \sin(f(k, s))e^{-\frac{s}{2}}\psi_2(e^{-s}k), \quad (5.46)$$

$$\hat{\psi}_2(k, s) = \cos(f(k, s))e^{-\frac{s}{2}}\psi_2(e^{-s}k) + \sin(f(k, s))e^{-\frac{s}{2}}\psi_1(e^{-s}k), \quad (5.47)$$

where $f(k, s)$ is the Bogoliubov angle. Replacing the fields in the Hamiltonian we obtain after some algebra:

$$H(s) = \int dk \left[k(\hat{\psi}_1^\dagger(k, s)\hat{\psi}_2(k, s) + \hat{\psi}_2^\dagger(k, s)\hat{\psi}_1(k, s)) + m(\hat{\psi}_1^\dagger(k, s)\hat{\psi}_1(k, s) - \hat{\psi}_2^\dagger(k, s)\hat{\psi}_2(k, s)) \right],$$

$$\begin{aligned}
&= \int dk \quad e^{-s} \left[2k(\sin(2f(k, s)) \cos(2f(k, s))) + m(\cos^2(2f(k, s)) - \sin^2(2f(k, s))) \right] \\
&\quad \times \left[\psi_1^\dagger(e^{-s}k) \psi_1(e^{-s}k) - \psi_2^\dagger(e^{-s}k) \psi_2(e^{-s}k) \right] \\
&\quad + e^{-s} \left[k(\cos^2(2f(k, s)) - \sin^2(2f(k, s))) - 2m(\sin(2f(k, s)) \cos(2f(k, s))) \right] \\
&\quad \times \left[\psi_1^\dagger(e^{-s}k) \psi_2(e^{-s}k) + \psi_2^\dagger(e^{-s}k) \psi_1(e^{-s}k) \right], \\
&= \int dk \quad e^{-s} \left[k \sin(2f(k, s)) + m \cos(2f(k, s)) \right] \left[\psi_1^\dagger(e^{-s}k) \psi_1(e^{-s}k) - \psi_2^\dagger(e^{-s}k) \psi_2(e^{-s}k) \right] \\
&\quad + e^{-s} \left[k \cos(2f(k, s)) - m \sin(2f(k, s)) \right] \left[\psi_1^\dagger(e^{-s}k) \psi_2(e^{-s}k) - \psi_1(e^{-s}k) \psi_2^\dagger(e^{-s}k) \right].
\end{aligned} \tag{5.48}$$

Now we find the energy functional, $E[\chi]$, by evaluating the inner product:

$$E[\chi] = \lim_{s_\xi \rightarrow -\infty} \langle \Omega | H(s_\xi) | \Omega \rangle. \tag{5.49}$$

We note at this point the nature of the ground state. Namely that ψ_1 is the annihilator of particles and ψ_2^\dagger is the annihilator of anti-particles, $\psi_1(x) |\Omega\rangle = 0 = \psi_2^\dagger(x) |\Omega\rangle$. With this in mind and defining $f(k) = \lim_{s_\xi \rightarrow -\infty} f(k, s_\xi)$ we obtain:

$$E[\chi] = - \int dk \delta(e^{-s}k - e^{-s}k) [k \sin(2f(k)) + m \cos(2f(k))] e^{-s}, \tag{5.50}$$

coming from the second term in the Hamiltonian. Noting that $\delta(\alpha x) = \frac{\delta(x)}{|\alpha|}$ and replacing the δ -function at zero by an infinite space integral we have:

$$e[\chi] = E[\chi] / \left(\int dx \right) = - \int \frac{dk}{2\pi} [k \sin(2f(k)) + m \cos(2f(k))]. \tag{5.51}$$

Before varying this functional with respect to χ recall the relation between $f(k, s)$ and $\chi(s)$.

$$\begin{aligned}
\frac{\partial}{\partial s} f(k, s) &= g(e^{-s}k, s), \\
g\left(\frac{k}{\Lambda}, s\right) &= \chi(s) \frac{k}{\Lambda} \Gamma\left(\frac{|k|}{\Lambda}\right), \\
\frac{\delta}{\delta \chi(s)} f(k) &= e^{-s} \frac{k}{\Lambda} \Gamma\left(e^{-s} \frac{|k|}{\Lambda}\right).
\end{aligned}$$

One may also notice the difference here between $g(k, u)$ for bosons and $g(k, u)$ for fermions - the additional factor of k/Λ from the lowest order polynomial term in k . Now we may take the variational derivative:

$$\begin{aligned}
\frac{\delta}{\delta \chi(s)} \frac{E[\chi]}{\int dx} &= \frac{\delta e[\chi]}{\delta \chi(s)} = \int \frac{dk}{2\pi} [k \cos(2f(k)) - m \sin(2f(k))] 2 \frac{\delta f(k)}{\delta \chi(s)}, \\
\frac{\delta e[\chi]}{\delta \chi(s)} &= \int \frac{dk}{2\pi} [k \cos(2f(k)) - m \sin(2f(k))] 2e^{-s} \frac{k}{\Lambda} \Gamma\left(e^{-s} \frac{|k|}{\Lambda}\right) = 0, \forall s \in (-\infty, 0].
\end{aligned} \tag{5.52}$$

Hence, we have the requirement that:

$$[k \cos(2f(k)) - m \sin(2f(k))] = 0, \forall k < \Lambda.$$

Solving easily for $f(k)$ one finds that:

$$f(k) = \frac{1}{2} \arctan\left(\frac{k}{m}\right),$$

which by use of an identity may be expressed as:

$$f(k) = \frac{1}{2} \arcsin\left[\frac{k}{\sqrt{k^2 + m^2}}\right], \forall k < \Lambda. \quad (5.53)$$

This result is compared with the following:

$$f(k) = \lim_{s_\xi \rightarrow -\infty} \int_0^{s_\xi} g(e^{-\omega}k, \omega) d\omega = - \int_0^\infty \chi(-\ln z) \frac{k}{\Lambda} \Theta(1 - z|k|/\Lambda) dz = -\frac{k}{\Lambda} \int_1^{\Lambda/|k|} \chi(-\ln z) dz,$$

where in the second equality we inserted the minimal form of g with the choice of a hard cut-off function. In addition the change of variables $z = e^{-\omega}$ is made. Now setting both forms of $f(k)$ equal to one another we find:

$$\int_1^{\Lambda/|k|} \chi(-\ln z) dz = -\frac{\Lambda}{2|k|} \arcsin\left[\frac{k}{\sqrt{k^2 + m^2}}\right]. \quad (5.54)$$

Then taking a derivative with respect to k on both sides we find the result:

$$\chi(s) = \kappa^2 \frac{d}{d\kappa} \frac{1}{2\kappa} \arcsin\left[\frac{\kappa}{\sqrt{\kappa^2 + (m/\Lambda)^2}}\right]_{\kappa=e^s}, \quad (5.55)$$

where we've used the dimensionless variable $\kappa = k/\Lambda$. As found in [8], eqn (123), we find then:

$$\chi(s) = \frac{1}{2} \left[-\arcsin \frac{\Lambda e^s}{\sqrt{\Lambda^2 e^{2s} + m^2}} + \frac{m\Lambda e^s}{\Lambda^2 e^{2s} + m^2} \right]. \quad (5.56)$$

For the massless case one immediately can see the result:

$$\begin{aligned} \chi(s) &= -\frac{1}{2} \arcsin\left(\frac{\Lambda e^s}{\Lambda e^s}\right), \\ &= -\frac{1}{2} \arcsin(+1) = -\frac{\pi}{4} \end{aligned} \quad (5.57)$$

Inserting this expression into the relation to the metric element yields a dual metric which is pure AdS².

As before it is worth making a sanity check for the energy density (5.51) in the massless case using the Bogoliubov angle (5.53) determine by variational method. Putting these together, one finds:

$$\begin{aligned} e[\chi] &= - \int \frac{dk}{2\pi} \left[k \sin\left(2\frac{1}{2} \arcsin\left[\frac{k}{\sqrt{k^2}}\right]\right) \right], \\ &= \int \frac{dk}{2\pi} \left[-k \left[\frac{k}{\sqrt{k^2}}\right] \right], \\ &= \int \frac{dk}{2\pi} (-k). \end{aligned} \quad (5.58)$$

²Up to a scaling of the real space as seen in the case of the scalar field.

5.4 Lifshitz Dirac I

A fermionic theory with anisotropic scaling will have the following Lagrangian in $(1+1)$ -dimensions:

$$\mathcal{L}_{Lifshitz} = \bar{\psi} \left(\hbar \gamma^t i \partial_t + \hbar \alpha \gamma^x (i \partial_x)^\nu - \mu \alpha^2 \right) \psi. \quad (5.59)$$

Some explanation is required of the variables now appearing in the Lagrangian. Firstly, we reintroduce the constants that would normally be set to one to make the dimensionality of terms more manifest. The α which appears is a skewed inverse speed of light. For $\nu = 1$, $\alpha = 1/c$, and in general α has units of m^ν/s . Similarly, μ is the skewed mass which in general has units of $kg/m^{2\nu-2}$. If $\nu = 1$ then we recover the units we usually have that are often set to one, as in the previous section. One might expect only the derivative to be exponentiated in the second term however, in order to preserve hermiticity the i must also be exponentiated. In this way one may repeatedly integrate by parts ν times to recover the original theory. Keeping the same matrix conventions as before, this yields the Fourier transformed Hamiltonian:

$$H = \int dk \left[-\hbar \alpha (-k)^\nu (\psi_1^\dagger(k) \psi_2(k) + \psi_2^\dagger(k) \psi_1(k)) + \mu \alpha^2 (\psi_1^\dagger(k) \psi_1(k) - \psi_2^\dagger(k) \psi_2(k)) \right]. \quad (5.60)$$

Following precisely the same steps as in Section (5.3) using this Hamiltonian one will find for the Bogoliubov angle:

$$f(k) = \frac{1}{2} \arcsin \left[\frac{-\hbar (-k)^\nu}{\sqrt{(-\hbar)^2 (-k)^{2\nu} + \alpha^2 \mu^2}} \right], \forall k < \Lambda. \quad (5.61)$$

From this we find that $\chi(s)$ is given by:

$$\chi(s) = \frac{k^2}{2} \frac{\partial}{\partial k} \frac{1}{k} \arcsin \left[\frac{-\hbar (-k)^\nu}{\sqrt{(-\hbar)^2 (-k)^{2\nu} + \alpha^2 \mu^2}} \right]_{k=\Lambda e^s}. \quad (5.62)$$

Evaluating this we obtain the following:

$$\chi(s) = -\frac{1}{2} \arcsin \left[\frac{-\hbar (-\Lambda e^s)^\nu}{\sqrt{(-\hbar)^2 (-\Lambda e^s)^{2\nu} + \alpha^2 \mu^2}} \right] - \frac{1}{2} \frac{\hbar \mu \alpha \nu (-\Lambda e^s)^\nu}{((-\hbar)^2 (-\Lambda e^s)^{2\nu} + \alpha^2 \mu^2)}. \quad (5.63)$$

The massless case is easily checked, the second term is zero and the first yields:

$$\begin{aligned} \chi(s) &= -\frac{1}{2} \arcsin \left[\frac{-\hbar (-\Lambda e^s)^\nu}{\sqrt{(-\hbar)^2 (-\Lambda e^s)^{2\nu}}} \right], \\ &= -\frac{1}{2} \arcsin[+1] = -\frac{\pi}{4}, \end{aligned}$$

which indeed is the result mentioned in the literature [8]. It would seem then that after turning the crank to find the entanglement entropy by Ryu-Takayanagi methods³ the result for a Dirac theory and a Lifshitz Dirac theory have no difference in entanglement up to a normalisation factor. However, it is suspected by the author that not only are even/odd values of ν different but also odd values yield theories with zero entanglement entropy.

³By which we mean, from χ calculating a geodesic length through the bulk geometry and so on as we performed in Section (5.2) for the scalar field.

5.5 Lifshitz Dirac II

We repeat the steps of the previous section with the standard γ matrix basis. Our expectation is that by changing basis we in effect redefined our fields as combinations of the original fields. This may be considered as a rotation of the field components which may in turn affect the Bogoliubov angle that we aim to find and which determines the function χ . So our conventions are now as follows:

$$\mathcal{L}_{Lifshitz} = \bar{\psi} (\hbar\gamma^t i\partial_t + \hbar\alpha\gamma^x (i\partial_x)^\nu - \mu\alpha^2) \psi, \quad (5.64)$$

$$H = - \int dx \bar{\psi} (\hbar\alpha\gamma^x (i\partial_x)^\nu - \mu\alpha^2) \psi, \quad (5.65)$$

$$\gamma^t = \begin{pmatrix} 0 & 1 \\ 1 & 0 \end{pmatrix}, \quad \gamma^x = \begin{pmatrix} 0 & -1 \\ 1 & 0 \end{pmatrix}, \quad \bar{\psi} = \psi^\dagger \gamma^t. \quad (5.66)$$

The remaining conventions apply, for the definition of $\bar{\psi}$ and so forth. From this point we expand in detail the Hamiltonian to find:

$$\begin{aligned} H &= - \int dx [\hbar\alpha\bar{\psi}\gamma^x(i\partial_x)^\nu\psi - \mu\alpha^2\bar{\psi}\psi], \\ &= - \int dx \left[\hbar\alpha \begin{pmatrix} \psi_1^\dagger & \psi_2^\dagger \end{pmatrix} \begin{pmatrix} 1 & 0 \\ 0 & -1 \end{pmatrix} \begin{pmatrix} (i\partial_x)^\nu\psi_1 \\ (i\partial_x)^\nu\psi_2 \end{pmatrix} - \mu\alpha^2 \begin{pmatrix} \psi_1^\dagger & \psi_2^\dagger \end{pmatrix} \begin{pmatrix} 0 & 1 \\ 1 & 0 \end{pmatrix} \begin{pmatrix} \psi_1 \\ \psi_2 \end{pmatrix} \right], \\ &= - \int dx \left[\hbar\alpha(\psi_1^\dagger(i\partial_x)^\nu\psi_1 - \psi_2^\dagger(i\partial_x)^\nu\psi_2) - \mu\alpha^2(\psi_1^\dagger\psi_2 + \psi_2^\dagger\psi_1) \right], \\ &= - \int dx \left[\hbar\alpha(\psi_1^\dagger(i\partial_x)^\nu\psi_1 - \psi_2^\dagger(i\partial_x)^\nu\psi_2) - \mu\alpha^2(\psi_1^\dagger\psi_2 + \psi_2^\dagger\psi_1) \right]. \end{aligned} \quad (5.67)$$

Now as before we Fourier transform the fields to obtain:

$$H = - \int dk \left[\hbar\alpha(-k)^\nu \left[\psi_1^\dagger(k)\psi_1(k) - \psi_2^\dagger(k)\psi_2(k) \right] - \mu\alpha^2 \left[\psi_1^\dagger(k)\psi_2(k) + \psi_2^\dagger(k)\psi_1(k) \right] \right]. \quad (5.68)$$

Next we perform a general Bogoliubov transformation in the same vein as [47], using the same transformation as in equations (5.46) and (5.47). After some algebra we find:

$$\begin{aligned} H &= - \int dk e^{-s} \\ &\quad \hbar\alpha(-k)^\nu \left[\cos(2f(k, s)) [\psi_1^\dagger(\tilde{k})\psi_1(\tilde{k}) - \psi_2^\dagger(\tilde{k})\psi_2(\tilde{k})] - \sin(2f(k, s)) [\psi_1^\dagger(\tilde{k})\psi_2(\tilde{k}) + \psi_2^\dagger(\tilde{k})\psi_1(\tilde{k})] \right], \\ &\quad - \mu\alpha^2 \left[\cos(2f(k, s)) [\psi_1^\dagger(\tilde{k})\psi_2(\tilde{k}) + \psi_2^\dagger(\tilde{k})\psi_1(\tilde{k})] + \sin(2f(k, s)) [\psi_1^\dagger(\tilde{k})\psi_1(\tilde{k}) - \psi_2^\dagger(\tilde{k})\psi_2(\tilde{k})] \right], \end{aligned}$$

where $e^{-s}k = \tilde{k}$ for brevity of presentation. Bringing similar terms together we have the final form we need to determine the Bogoliubov angle $f(k)$:

$$\begin{aligned} H &= - \int dk e^{-s} \left[[\hbar\alpha(-k)^\nu \cos(2f(k, s)) - \mu\alpha^2 \sin(2f(k, s))] [\psi_1^\dagger(\tilde{k})\psi_1(\tilde{k}) - \psi_2^\dagger(\tilde{k})\psi_2(\tilde{k})] \right] \\ &\quad - \left[[\hbar\alpha(-k)^\nu \sin(2f(k, s)) + \mu\alpha^2 \cos(2f(k, s))] [\psi_1^\dagger(\tilde{k})\psi_2(\tilde{k}) - \psi_2^\dagger(\tilde{k})\psi_1(\tilde{k})] \right]. \end{aligned} \quad (5.69)$$

From this we determine the energy functional from $\langle \Omega | H | \Omega \rangle$ keeping in mind the action of the field operators on the unentangled IR state $|\Omega\rangle$ as in equation (5.49) and the paragraph thereafter.

$$E[\chi] = - \int dk e^{-s} (-1) [\hbar\alpha(-k)^\nu \cos(2f(k)) - \mu\alpha^2 \sin(2f(k))] \delta(e^{-s}k - e^{-s}k),$$

$$= \int dx \int \frac{dk}{2\pi} [\hbar\alpha(-k)^\nu \cos(2f(k)) - \mu\alpha^2 \sin(2f(k))]. \quad (5.70)$$

Taking the functional derivative as previously shown yields:

$$\frac{\delta e[\chi]}{\delta \chi(s)} = \int \frac{dk}{2\pi} [-\hbar\alpha(-k)^\nu \sin(2f(k)) - \mu\alpha^2 \cos(2f(k))] 2e^{-s} \frac{k}{\Lambda} \Gamma\left(e^{-s} \frac{|k|}{\Lambda}\right) = 0, \forall s \in (-\infty, 0].$$

This gives the following expression for the angle $f(k)$:

$$f(k) = \frac{1}{2} \arctan \left[\frac{\mu\alpha}{-\hbar(-k)^\nu} \right]. \quad (5.71)$$

Using a couple of identities we can express this as:

$$\begin{aligned} f(k) &= \frac{1}{2} \arctan \left[\frac{\hbar(-k)^\nu}{\mu\alpha} \right] \mp \frac{\pi}{4}, \\ &= \frac{1}{2} \arcsin \left[\frac{\hbar(-k)^\nu}{\sqrt{(-\hbar)^2(-k)^{2\nu} + \mu^2\alpha^2}} \right] \mp \frac{\pi}{4}. \end{aligned} \quad (5.72)$$

where we take the minus for ν even and plus for ν odd, not by choice but by conditions required by the identities used. It remains to find $\chi(s)$ which will be given by:

$$\begin{aligned} \chi(s) &= f(k) - k\partial_k f(k)|_{k=\Lambda e^s}, \\ &= \mp \frac{\pi}{4} + \frac{1}{2} \arcsin \left(\frac{\hbar(-k)^\nu}{\sqrt{(-\hbar)^2(-k)^{2\nu} + \mu^2\alpha^2}} \right) - \frac{1}{2} \frac{\hbar\nu\mu\alpha(-k)^\nu}{((-\hbar)^2(-k)^{2\nu} + \mu^2\alpha^2)} \Big|_{k=\Lambda e^s}, \end{aligned} \quad (5.73)$$

$$= \mp \frac{\pi}{4} + \frac{1}{2} \arcsin \left(\frac{\hbar}{\sqrt{(-\hbar)^2 + M(s, \nu)^2}} \right) - \frac{1}{2} \frac{\hbar\nu M(s, \nu)}{((-\hbar)^2 + M(s, \nu)^2)}, \quad (5.74)$$

where we've defined $M(s, \nu) := \frac{\mu\alpha}{(-\Lambda e^s)^\nu}$.

For $M(s, \nu) = 0$ we find two results:

$$\chi(s) = \begin{cases} \frac{\pi}{2}, & \nu \text{ odd,} \\ 0, & \nu \text{ even.} \end{cases} \quad (5.75)$$

So for the entropy we find that we recover the log correction for odd values of nu but *no* entanglement for even value. While this may come as a surprising, even counter-intuitive, result recent result using numerical field theoretic methods seems to confirm this prediction [59]. So while further physical explanation is necessary we currently have evidence from alternative methods which seem to repeat the same prediction.

For the massive case we can look at the $\nu = 1 = \hbar = \alpha$ case as a sanity check to find:

$$\chi(s) = \frac{\pi}{4} - \frac{1}{2} \arcsin \left(\frac{k}{\sqrt{k^2 + m^2}} \right) + \frac{1}{2} \frac{mk}{(k^2 + m^2)} \Big|_{k=\Lambda e^s}, \quad (5.76)$$

which up to the constant factor of $\frac{\pi}{4}$ is precisely the result obtained in [8]. It would seem that the effect of choosing the standard basis is that the Bogoliubov angle has been shifted by $\frac{\pi}{4}$. With the energy density and Bogoliubov angle determined we can perform a check on the ground state energy density. In the massless case, combining (5.70) and (5.72) gives for ν odd:

$$e[\chi] = E[\chi]/\left(\int dx\right) = \int \frac{dk}{2\pi} [\hbar\alpha(-k)^\nu \cos(\pi)], \quad (5.77)$$

$$= \int \frac{dk}{2\pi} [\hbar\alpha k^\nu], \quad (5.78)$$

and for ν even:

$$e[\chi] = \int \frac{dk}{2\pi} [\hbar\alpha(-k)^\nu \cos(0)], \quad (5.79)$$

$$= \int \frac{dk}{2\pi} [\hbar\alpha k^\nu]. \quad (5.80)$$

To compare to Section(5.4) where according to⁴ [47] the energy is given by:

$$E[\chi]/(\int dx) = - \int \frac{dk}{2\pi} [\hbar\alpha(-k)^\nu \sin(2f(k)) + \mu\alpha^2 \cos(2f(k))], \quad (5.81)$$

and

$$f(k) = \frac{\pi}{4} \quad \forall k, \nu. \quad (5.82)$$

Then in the massless case we have:

$$e[\chi] = - \int \frac{dk}{2\pi} [\hbar\alpha(-k)^\nu \sin\left(\frac{\pi}{2}\right)] = - \int \frac{dk}{2\pi} [\hbar\alpha(-k)^\nu] = \int \frac{dk}{2\pi} \hbar\alpha k^\nu \quad \forall \nu. \quad (5.83)$$

Thus we have an agreement between the two approaches, at least at the level of the ground state. However, interestingly the deviation in Bogoliubov angle and hence the function χ leads to a difference in entanglement entropy for both approaches when we proceed to calculate the entanglement entropy using Ryu-Takayanagi. At this point we can only say with certainty that the result (5.75) is a prediction for anisotropic fermionic theories.

A question remains as to why precisely the function χ differs due to a different choice of γ -matrix. We put forward that a possible explanation to this point is that the unentangled reference state $|\Omega\rangle$ is not the same in both cases. As such the nature of the entanglement in the resultant UV limit of the cMERA state $|\Psi\rangle$ is different. If the choice of γ -matrices is considered as a redefinition of the spinor components then the definition of the reference state changes with either choice. The confirmation of the result by field theoretic methods and a further explanation of the above question remain as paths for future study.

⁴See the appendix of version 1, equation (51)

Chapter 6

Conclusion

Here we make some concluding remarks regarding the MERA, cMERA techniques and the main result of the previous chapter.

Evidently as outlined as a numerical technique MERA is effective in simulating 1-dimensional systems. While some tensor networks are more numerically efficient the MERA possesses valuable properties which make it particularly useful in acting as an analogue to 1-dimensional systems. The entanglement entropy bound for MERA which reproduces the known entropy bounds for scale invariant systems is of special interest. While MPS states have a similar entropy bound, the bound of MERA can be enveloped into the overarching Ryu-Takayanagi proposal. We can view the bound as a minimisation of geodesics in the bulk or network dimension.

Now taking this idea in mind the study of MERA can be extended from a numerical procedure to an intermediary theory which can connect seemingly disparate areas of physics. This in itself warrants a deep study of the ansatz as it would be of great benefit to understand further how a discrete space can be generated from a many-body quantum system and if entanglement itself builds space-time [31, 52].

If we move past the big question of if entanglement builds space-time we can use cMERA techniques to study field theories. In this thesis we have examined free field theories both scalar and fermionic in the cMERA framework. In this examination we focused of course on entanglement entropy. Moreover, we extended previous work to those theories with Lifshitz scaling. In doing so we have produced a validation of cMERA techniques applied to these theories. Questions remain regarding the final result. One expects that the result may be verified using purely field theoretic methods, as mentioned at the moment numerical evidence [59] supports our prediction but a full explanation is still required. We would propose this as promising path for future inquiry. Some ignorance remains as to why this result does not manifest itself using alternate conventions as appear in the literature.

There is a huge number of possibilities for future research in the area of MERA and AdS/MERA. There are proposals for the study of AdS black holes using finite temperature MERA [60]. As we have hinted at there is some speculation in the area of quantum gravity. Perhaps a more immediate case for further study is the use of MERA and cMERA techniques in the classification of quantum many-body systems by their emergent bulk geometries. Specifically for the cMERA framework itself it would be interesting to examine the results generated by more general disentangling operators. In our treatment we used perhaps the most straightforward form of the disentangler \hat{K} , that is one with only s -wave momentum dependence.

Appendix A

Quantum Information

A.1 Qubits

A qubit is a two dimensional Hilbert space $\mathcal{H}^2 \simeq \mathbb{C}^2$ where the qubit values take the form:

$$|\phi\rangle = c_0 |0\rangle + c_1 |1\rangle, \quad (\text{A.1})$$

where $\{|0\rangle, |1\rangle\}$ is an orthonormal set called the standard computational basis, $c_0, c_1 \in \mathbb{C}$ and $|c_0|^2 + |c_1|^2 = 1$. Physically these qubits could correspond to spin up/down states in a spin basis.

For larger systems of say n qubits, or indeed n particles which we describe using the computational or a related basis, the corresponding Hilbert space is given by the tensor product of individual 2-dimensional Hilbert spaces:

$$\bigotimes_{i=1}^n \mathcal{H}^2 = \mathcal{H}^2 \otimes \mathcal{H}^2 \cdots \otimes \mathcal{H}^2 = \mathcal{H}^{2^n}. \quad (\text{A.2})$$

Then for example we have the states:

$$\begin{aligned} |\phi_1\rangle &= |0\rangle \otimes |0\rangle = |00\rangle, \\ |\phi_2\rangle &= \frac{1}{\sqrt{2}}(|0\rangle + |1\rangle) \otimes |0\rangle = \frac{1}{\sqrt{2}}(|00\rangle + |10\rangle), \\ |\phi_3\rangle &= \frac{1}{\sqrt{2}}(|00\rangle + |11\rangle) \neq |A\rangle \otimes |B\rangle, \end{aligned} \quad (\text{A.3})$$

which are all in the Hilbert space \mathcal{H}^{2^2} of 2-qubit states. Moreover the first two are examples of separable/product states and the third is a non-separable or *entangled* state. The meaning of this statement will be explain at length later.

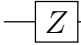
A.2 Quantum Gates

Operations on these qubit bases are regarded as quantum logic operations in analogy with classical computation logic operations. In this context the operations are given by unitary operations acting on the qubit Hilbert space. Being unitary all the operations are thus reversible.

Now we give some examples of the unitary operators or quantum gates which act on such states.

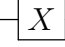
Phase Flip (\hat{Z}) gate which we can define by its operation on single qubits.

$$\begin{aligned} \hat{Z} |0\rangle &= |0\rangle, \\ \hat{Z} |1\rangle &= -|1\rangle. \end{aligned} \quad (\text{A.4})$$

In circuit diagram notation this is: . In matrix notation this is σ^z .

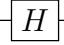
Bit Flip (\hat{X}) gate

$$\begin{aligned}\hat{X} |0\rangle &= |1\rangle, \\ \hat{X} |1\rangle &= |0\rangle.\end{aligned}\tag{A.5}$$

In circuit diagram notation this is: . In matrix notation this is σ^x .

Hadamard (Rotation) (\hat{H}) gate

$$\begin{aligned}\hat{H} |0\rangle &= \frac{1}{\sqrt{2}}(|0\rangle + |1\rangle), \\ \hat{H} |1\rangle &= \frac{1}{\sqrt{2}}(|0\rangle - |1\rangle).\end{aligned}\tag{A.6}$$

In circuit diagram notation this is: . In matrix notation this is $\frac{1}{\sqrt{2}}(\sigma^x + \sigma^z)$. At this point we can also describe gates which act on several qubits at once. **CNOT** gate. In classical computation this may be called an XOR (exclusive OR) operation. It acts on two qubits using the first as control-qubit and the second as the registry qubit.

$$\begin{aligned}CNOT |00\rangle &= |00\rangle, \\ CNOT |01\rangle &= |01\rangle, \\ CNOT |10\rangle &= |11\rangle, \\ CNOT |11\rangle &= |10\rangle.\end{aligned}\tag{A.7}$$

There is some more notation to keep in mind for this gate. While acting on 2 qubits they may not need to be adjacent so we denote the relevant qubits for a particular *CNOT*-gate by using a pair of indices like so: $CNOT_{ij}$. The meaning of this is to say that the control qubit is the i^{th} qubit of the circuit and the target/registry qubit is the j^{th} qubit. For the defining example above we would denote the gate by $CNOT_{12}$ and use the diagram below:

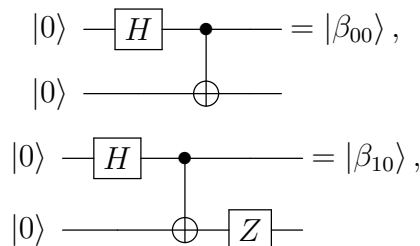


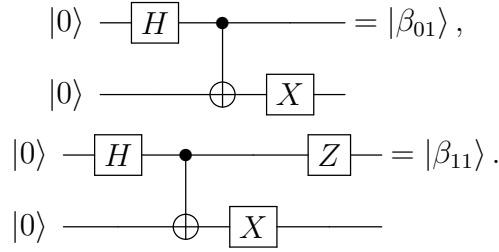
A.3 Quantum Circuits

Using the simple examples that we have so far we can construct our first quantum circuit which will give us a method of translating a 2-qubit computational basis $\{|00\rangle, |01\rangle, |10\rangle, |11\rangle\}$ to another 2-qubit basis called the Bell basis: $\{|\beta_{00}\rangle, |\beta_{01}\rangle, |\beta_{10}\rangle, |\beta_{11}\rangle\}$, where:

$$\begin{aligned}|\beta_{00}\rangle &= \frac{1}{\sqrt{2}}(|00\rangle + |11\rangle), & |\beta_{10}\rangle &= \frac{1}{\sqrt{2}}(|00\rangle - |11\rangle), \\ |\beta_{01}\rangle &= \frac{1}{\sqrt{2}}(|01\rangle + |10\rangle), & |\beta_{11}\rangle &= \frac{1}{\sqrt{2}}(|01\rangle - |10\rangle).\end{aligned}\tag{A.8}$$

So the circuits to translate between these bases are:





The right-hand side of these circuits denote a total output of the Bell states not one single leg giving a Bell state. Moreover, we have implicitly taken that a single qubit (\hat{A}) gate operates as a two qubit gate as: $(\hat{A} \otimes \hat{\mathbb{I}}) = \hat{A}_1$. So in fact the above circuits may be also expressed as:

$$\begin{aligned}
|\beta_{00}\rangle &= CNOT_{12}(\hat{H} \otimes \hat{\mathbb{I}}) |00\rangle = CNOT_{12}\hat{H}_1 |00\rangle, \\
|\beta_{10}\rangle &= (\hat{\mathbb{I}} \otimes \hat{Z})CNOT_{12}(\hat{H} \otimes \hat{\mathbb{I}}) |00\rangle = \hat{Z}_2CNOT_{12}\hat{H}_1 |00\rangle, \\
|\beta_{01}\rangle &= (\hat{\mathbb{I}} \otimes \hat{X})CNOT_{12}(\hat{H} \otimes \hat{\mathbb{I}}) |00\rangle = \hat{X}_2CNOT_{12}\hat{H}_1 |00\rangle, \\
|\beta_{11}\rangle &= (\hat{Z} \otimes \hat{\mathbb{I}})(\hat{\mathbb{I}} \otimes \hat{X})CNOT_{12}(\hat{H} \otimes \hat{\mathbb{I}}) |00\rangle = \hat{Z}_1\hat{X}_2CNOT_{12}\hat{H}_1 |00\rangle.
\end{aligned} \tag{A.9}$$

We can take the other computational basis states as inputs and find the Bell states in a similar fashion. The above circuits we refer to as the Bell state generator. For simplicity of the realisation of such a circuit we tend to want to use the same inputs states, say light of a certain polarization, so in the end we can modify only the end of the circuit rather than having a different circuit for every input.

A.4 States and Representations

We note that the basis states for the qubits in the quantum information context reside in a state space called the Hilbert space, \mathcal{H} . We should note here some defining properties of the state space before we go on to give properties of the states.

- The state space is a vector space over the field \mathbb{C} .
- It has an inner product which we denote by $\langle \cdot | \cdot \rangle$
- This inner product induces a norm and metric on the space.
- In the infinite dimensional case the space is also complete.

So in particular we use $|v\rangle$ to denote a vector/state in the Hilbert space and then $\langle v|$ denotes the adjoint of this vector/state.

Norm: If we take two states, $|\phi_i\rangle, |\phi_j\rangle$, such that $\langle \phi_i | \phi_j \rangle = \delta_{ij}$ then we define the norm as:

$$\langle \phi_i | \phi_i \rangle^{\frac{1}{2}} = norm(\phi_i) \in \mathbb{C},$$

where $norm(\phi_i) = 1$ for a normalized state.

Metric: A metric, $\rho(\cdot, \cdot)$, on a space is defined by the following properties:

- $\rho(|\phi\rangle, |\psi\rangle) = 0, \iff |\phi\rangle = |\psi\rangle,$
- $\rho(|\phi\rangle, |\psi\rangle) = \rho(|\psi\rangle, |\phi\rangle),$
- $\rho(|\phi\rangle, |\xi\rangle) \leq \rho(|\psi\rangle, |\phi\rangle) + \rho(|\phi\rangle, |\xi\rangle),$

where $|\phi\rangle, |\psi\rangle, |\xi\rangle \in \mathcal{H}$. Then for the metric to be induced by the norm we should find that:

$$\rho(|\phi\rangle, |\psi\rangle) = \|\phi - \psi\|.$$

Representations: We should try to be more precise in what we mean by the states we denote by the kets above. Suppose we have a Hilbert space \mathcal{H} with a basis given by $\mathcal{B} = \{|\phi_i\rangle\}_{i \geq 1}$. Suppose also we have that $|\psi\rangle \in \mathcal{H}$. Then using the completeness relation for a basis set: $\sum_{i \geq 1} |\phi_i\rangle \langle \phi_i| = \hat{\mathbb{I}}$ we have that:

$$\begin{aligned} |\psi\rangle &= \sum_{i \geq 1} |\phi_i\rangle \langle \phi_i | \psi \rangle, \\ &= \sum_{i \geq 1} |\phi_i\rangle c_{\psi}^i, \\ &= \sum_{i \geq 1} c_{\psi}^i |\phi_i\rangle, \end{aligned} \tag{A.10}$$

where c_{ψ}^i are complex numbers corresponding to the inner products of the basis states with the state in question. So in particular the state $|\psi\rangle$ is expressed as a superposition of basis states. This is what we mean by a state in our Hilbert space. For example, with the computational basis we have the following data:

$$\begin{aligned} \mathcal{B} &= \{|0\rangle, |1\rangle\}, \quad |\psi\rangle \in \mathcal{H}, \\ |\psi\rangle &= \sum_{i=0}^1 c_i |i\rangle, \\ &= c_0 |0\rangle + c_1 |1\rangle. \end{aligned} \tag{A.11}$$

Likewise if we look at the Hilbert space of two qubit states we have:

$$\begin{aligned} \mathcal{B} &= \{|00\rangle, |01\rangle, |10\rangle, |11\rangle\}, & \mathcal{B}_{Bell} &= \{|\beta_{00}\rangle, |\beta_{01}\rangle, |\beta_{10}\rangle, |\beta_{11}\rangle\}, \\ |\psi\rangle &= \sum_{i,j=0}^1 c_{ij} |ij\rangle, & \text{OR: } |\psi\rangle &= \sum_{i,j=0}^1 b_{ij} |\beta_{ij}\rangle, \\ &= c_{00} |00\rangle + c_{01} |01\rangle + c_{10} |10\rangle + c_{11} |11\rangle, & &= b_{00} |\beta_{00}\rangle + b_{01} |\beta_{01}\rangle + b_{10} |\beta_{10}\rangle + b_{11} |\beta_{11}\rangle. \end{aligned} \tag{A.12}$$

We can see more clearly here that the Bell states form a basis as we can see from their expressions given previously that they may be written as a superposition of the computational basis states and most importantly they are mutually orthogonal states so they span the entire Hilbert space. Moreover we note that the two qubit Hilbert space is given by the tensor product of two 1-qubit Hilbert spaces. What we mean by this is that for two vector spaces \mathcal{U} and \mathcal{V} the tensor product of these two spaces is a vector space, $\mathcal{W} = \mathcal{U} \otimes \mathcal{V}$, of dimension $(\dim \mathcal{U} \cdot \dim \mathcal{V})$. Taking the bases of these spaces to be $\mathcal{B}_{\mathcal{U}} = \{|u_1\rangle, |u_2\rangle \dots\}$ and $\mathcal{B}_{\mathcal{V}} = \{|v_1\rangle, |v_2\rangle \dots\}$ respectively, then the basis of \mathcal{W} is $\mathcal{B}_{\mathcal{W}} = \{|u_1 v_1\rangle, |u_1 v_2\rangle \dots\}$, where $|u_i v_j\rangle = |u_i\rangle \otimes |v_j\rangle$. You can check this quickly for the above examples.

Appendix B

Bibliography

- [1] Einstein, A., Podolsky, B. & Rosen, N. Can quantum-mechanical description of physical reality be considered complete? *Phys. Rev.* **47**, 777–780 (1935). URL <https://link.aps.org/doi/10.1103/PhysRev.47.777>.
- [2] Bell, J. S. On the Einstein-Podolsky-Rosen paradox. *Physics* **1**, 195–200 (1964).
- [3] White, S. R. Density matrix formulation for quantum renormalization groups. *Phys. Rev. Lett.* **69**, 2863–2866 (1992). URL <https://link.aps.org/doi/10.1103/PhysRevLett.69.2863>.
- [4] Schollwöck, U. The density-matrix renormalization group in the age of matrix product states. *Annals of Physics* **326**, 96–192 (2011). [1008.3477](https://doi.org/10.1008.3477).
- [5] Verstraete, F., Cirac, J. I. & Murg, V. Matrix Product States, Projected Entangled Pair States, and variational renormalization group methods for quantum spin systems 1–99 (2009). URL <https://arxiv.org/abs/0907.2796v1>.
- [6] Swingle, B. Entanglement renormalization and holography. *Physical Review D - Particles, Fields, Gravitation and Cosmology* **86**, 1–8 (2012). [0905.1317](https://doi.org/10.1103/PhysRevD.86.090501).
- [7] Haegeman, J., Cirac, J. I., Osborne, T. J., Verschelde, H. & Verstraete, F. Applying the variational principle to (1+1)-Dimensional quantum field theories. *Physical Review Letters* **105**, 1–4 (2010). URL <https://arxiv.org/abs/1006.2409>. One should examine v1.
- [8] Nozaki, M., Ryu, S. & Takayanagi, T. Holographic geometry of entanglement renormalization in quantum field theories. *Journal of High Energy Physics* **2012** (2012). [1208.3469](https://doi.org/10.1088/1126-6708/2012/01/014).
- [9] Hartmann, D. Master Thesis: Sublattice entanglement entropy for fermions (2017).
- [10] Brynjolfsson, E. J., Danielsson, U. H., Thorlacius, L. & Zingg, T. Holographic models with anisotropic scaling. *Journal of Physics: Conference Series* **462**, 012055 (2013). URL <http://stacks.iop.org/1742-6596/462/i=1/a=012055>.
- [11] Baggio, M., de Boer, J. & Holsheimer, K. Anomalous breaking of anisotropic scaling symmetry in the quantum lifshitz model. *Journal of High Energy Physics* **2012**, 99 (2012). URL [https://doi.org/10.1007/JHEP07\(2012\)099](https://doi.org/10.1007/JHEP07(2012)099).
- [12] Son, D. & Wingate, M. General coordinate invariance and conformal invariance in non-relativistic physics: Unitary fermi gas. *Annals of Physics* **321**, 197 – 224 (2006). URL <http://www.sciencedirect.com/science/article/pii/S0003491605001958>.

- [13] de Boer, J., Hartong, J., Obers, N. A., Sybesma, W. & Vandoren, S. Perfect Fluids (2017). URL <http://arxiv.org/abs/1710.04708>.
- [14] de Boer, J., Hartong, J., Obers, N. A., Sybesma, W. & Vandoren, S. Hydrodynamic Modes of Homogeneous and Isotropic Fluids (2017). URL <http://arxiv.org/abs/1710.06885>.
- [15] Ryu, S. & Takayanagi, T. Holographic derivation of entanglement entropy from the anti-de sitter space/conformal field theory correspondence. *Phys. Rev. Lett.* **96**, 181602 (2006). URL <https://link.aps.org/doi/10.1103/PhysRevLett.96.181602>.
- [16] Ryu, S. & Takayanagi, T. Aspects of holographic entanglement entropy. *Journal of High Energy Physics* **2006**, 045 (2006). URL <http://stacks.iop.org/1126-6708/2006/i=08/a=045>.
- [17] Nielsen, M. A. & Chuang, I. L. Quantum Computation and Quantum Information (2000). URL <http://www.michaelnielsen.org/qcqi/>.
- [18] Preskill, J. Quantum computation. Lecture Notes: <http://www.theory.caltech.edu/people/preskill/ph229/> (10/10/2016).
- [19] Araki, H. & Lieb, E. H. Entropy inequalities. *Comm. Math. Phys.* **18**, 160–170 (1970). URL <https://projecteuclid.org:443/euclid.cmp/1103842506>.
- [20] Hastings, M. B. Entropy and entanglement in quantum ground states. *Physical Review B - Condensed Matter and Materials Physics* **76**, 1–7 (2007). [0701055](https://doi.org/10.1103/PhysRevB.76.070105).
- [21] Eisert, J., Cramer, M. & Plenio, M. B. Colloquium: Area laws for the entanglement entropy. *Reviews of Modern Physics* **82**, 277–306 (2010). [0808.3773](https://doi.org/10.1103/RevModPhys.82.277).
- [22] Wen, X. *et al.* Holographic entanglement renormalization of topological insulators. *Physical Review B* **94** (2016). URL <https://arxiv.org/abs/1605.07199>.
- [23] Franco-Rubio, A. & Vidal, G. Entanglement and correlations in the continuous multi-scale renormalization ansatz (2017). URL <http://arxiv.org/abs/1706.02841>. [1706.02841](https://doi.org/10.1103/PhysRevLett.118.028401).
- [24] Bao, N. *et al.* Consistency Conditions for an AdS/MERA Correspondence 1–38 (2015). [arXiv:1504.06632v1](https://arxiv.org/abs/1504.06632).
- [25] Czech, B., Lamprou, L., McCandlish, S. & Sully, J. Tensor networks from kinematic space. *Journal of High Energy Physics* **2016** (2016). [1512.01548](https://doi.org/10.1186/1029-2755-2016-1512).
- [26] Evenbly, G. & Vidal, G. Algorithms for Entanglement Renormalization: Boundaries, Impurities and Interfaces. *Journal of Statistical Physics* **157**, 931–978 (2014). [0707.1454](https://doi.org/10.1007/s10954-014-0145-4).
- [27] Evenbly, G. & Vidal, G. Tensor Network Renormalization. *Physical Review Letters* **115**, 1–6 (2015).
- [28] Evenbly, G. Algorithms for tensor network renormalization. *Physical Review B - Condensed Matter and Materials Physics* **95**, 1–21 (2017).
- [29] Vidal, G. Efficient simulation of one-dimensional quantum many-body systems 1–4 (2003). URL <http://dx.doi.org/10.1103/PhysRevLett.93.040502>. [0310089](https://doi.org/10.1103/PhysRevLett.93.040502).
- [30] Orus, R. A Practical Introduction to Tensor Networks: Matrix Product States and Projected Entangled Pair States 1–51 (2013). URL <http://dx.doi.org/10.1016/j.aop.2014.06.013>. [1306.2164](https://doi.org/10.1016/j.aop.2014.06.013).

- [31] Evenbly, G. & Vidal, G. Tensor Network States and Geometry. *Journal of Statistical Physics* **145**, 891–918 (2011). URL <https://arxiv.org/abs/1106.1082>. 1106.1082.
- [32] Swingle, B. Constructing holographic spacetimes using entanglement renormalization **02138** (2012). URL <http://arxiv.org/abs/1209.3304>.
- [33] Vidal, G. Entanglement Renormalization: an introduction (2009). URL <http://arxiv.org/abs/0912.1651>.
- [34] Evenbly, G. Foundations and Applications of Entanglement Renormalization (2010). URL <http://arxiv.org/abs/1109.5424v1>.
- [35] Vidal, G. A class of quantum many-body states that can be efficiently simulated. *Quantum* **4** (2006). URL <http://arxiv.org/abs/quant-ph/0610099>.
- [36] Penrose, R. *The Road to Reality: A Complete Guide to the Laws of the Universe*. Vintage Series (Vintage Books, 2007). URL <https://books.google.nl/books?id=coahAAAACAAJ>.
- [37] Biamonte, J., Bergholm, V. & Lanzagorta, M. Tensor network methods for invariant theory. *Journal of Physics A: Mathematical and Theoretical* **46**, 475301 (2013). URL <http://stacks.iop.org/1751-8121/46/i=47/a=475301>.
- [38] Pérez-García, D., Verstraete, F., Wolf, M. M. & Cirac, J. I. Matrix Product State Representations. *Quantum Inf. Comp.* **7**, 401 (2007). URL <https://arxiv.org/abs/quant-ph/0608197>.
- [39] Vidal, G. Entanglement renormalization. *Physical Review Letters* **99**, 1–4 (2007). 0512165.
- [40] Bény, C. Causal structure of the entanglement renormalization ansatz. *New Journal of Physics* **15** (2013). URL <https://arxiv.org/abs/1110.4872>. 1110.4872.
- [41] Corboz, P. Delta itp - advanced topics in theoretical physics i: Tensor networks. Unpublished Lectures (2017).
- [42] Evenbly, G. & Vidal, G. Quantum Criticality with the Multi-scale Entanglement Renormalization Ansatz (2011). URL <http://arxiv.org/abs/1109.5334>.
- [43] Cincio, L. Strongly Correlated Systems. *Dissertation* (2010).
- [44] Evenbly, G. & Vidal, G. Frustrated antiferromagnets with entanglement renormalization: Ground state of the spin-1/2 heisenberg model on a kagome lattice. *Physical Review Letters* **104**, 1–6 (2010).
- [45] Evenbly, G. & Vidal, G. Tensor Network Renormalization (2014). URL <http://dx.doi.org/10.1103/PhysRevLett.115.180405>.
- [46] Hauru, M. Multiscale Entanglement Renormalisation Ansatz. *Dissertation* (2013).
- [47] Haegeman, J., Osborne, T. J., Verschelde, H. & Verstraete, F. Entanglement renormalization for quantum fields in real space. *Physical Review Letters* **110**, 1–5 (2013). 1102.5524.
- [48] Vidal, G. Tensor Networks (presentation). In *It from Qubit* (2016).
- [49] Maldacena, J. The Large N Limit of Field Theories and Gravity (2000). URL <https://arxiv.org/abs/hep-th/9711200>.

- [50] Witten, E. Anti-de Sitter space and holography. *Adv. Theor. Math. Phys.* **2**, 253–291 (1998). URL <https://arxiv.org/abs/hep-th/9802150>.
- [51] Gubser, S., Klebanov, I. & Polyakov, A. Gauge theory correlators from non-critical string theory. *Physics Letters B* **428**, 105 – 114 (1998). URL <http://www.sciencedirect.com/science/article/pii/S0370269398003773>.
- [52] Raamsdonk, M. V. Lectures on Gravity and Entanglement 75 (2016). URL <http://arxiv.org/abs/1609.00026>.
- [53] de Boer, J., Verlinde, E. P. & Verlinde, H. L. On the holographic renormalization group. *JHEP* **08**, 003 (2000). URL <https://arxiv.org/abs/hep-th/9912012>.
- [54] Pfeifer, R. N. C., Evenbly, G. & Vidal, G. Entanglement renormalization, scale invariance, and quantum criticality. *Phys. Rev. A* **79**, 040301 (2009). URL <https://link.aps.org/doi/10.1103/PhysRevA.79.040301>.
- [55] He, T., Magan, J. M. & Vandoren, S. Entanglement Entropy in Lifshitz Theories I (2017). URL <http://arxiv.org/abs/1705.01147>.
- [56] Gentle, S. A. & Vandoren, S. Lifshitz entanglement entropy from holographic cMERA (2017). URL <http://arxiv.org/abs/1711.11509>.
- [57] Casini, H. & Huerta, M. Entanglement and alpha entropies for a massive scalar field in two dimensions. *Journal of Statistical Mechanics: Theory and Experiment* **2005**, P12012 (2005). URL <http://stacks.iop.org/1742-5468/2005/i=12/a=P12012>.
- [58] Calabrese, P. & Cardy, J. Entanglement entropy and quantum field theory. *Journal of Statistical Mechanics: Theory and Experiment* **2004**, P06002 (2004). URL <http://stacks.iop.org/1742-5468/2004/i=06/a=P06002>.
- [59] Hartmann, D. In preparation (2017).
- [60] Matsueda, H., Ishihara, M. & Hashizume, Y. Tensor network and a black hole. *Phys. Rev. D* **87**, 066002 (2013). URL <https://link.aps.org/doi/10.1103/PhysRevD.87.066002>.